# 8 Particle-stabilized foams

> These motions were such as to satisfy me, after frequently repeated observation, that they arose neither from currents in the fluid, nor from its gradual evaporation, but belonged to the particle itself.
>
> "Microscopical Observations on the Particles Contained in the Pollen of Plants," by Robert Brown, *Philosophical Magazine,* NS 4, 162–3, 1828.

## 8.1 Introduction

Partially hydrophobic small particles have the potential to act as stabilizing agents in many foaming processes, and they behave fairly similar in some ways to chemical surfactant molecules in that they can adsorb (attach) at the bubble interface. However, particles show several distinct differences from chemical surfactants. For example, macro-sized particles are considerably larger than the molecular dimensions exhibited by chemical surfactants. They also behave differently, in that particles cannot aggregate at the interface and are unable to buildup self-assembles and cannot solubilize in the bulk solution. Unlike chemical surfactants, it is difficult to generate bubbles or foams solely without particles, but partially hydrophobic particles can be good foam stabilizers at moderate concentrations (about 1 w%). In fact, if the particles exhibit moderate hydrophobicity, then the foams can be extremely stable (with lifetimes of the order of years). However, generally it is more convenient to add other surface-active components to the particles, such as polymers, dispersants or chemical surfactants, to ensure a higher degree of foamability and foam stability. The different features exhibited by surfactant- and particle-stabilized systems are illustrated in Fig. 8.1.

There are only a few foaming processes operating solely with particles, for example, molten metal foams (where ceramic particles are used) and sometimes hydrophobic particles (such as graphite) in the froth flotation process. Excluding the past two decades, the literature on foams stabilized by particles is sparse, but there has been a revival of attention, which was mostly because of the success achieved with particle-stabilized emulsions (Pickering emulsions). For a considerable period of time it has been well known that particles acted as stabilizers in many established industrial foaming processes, such as froth flotation of mineral particles (1), deinking flotation (2) and food processing (3). However, little effort was made to understand the mechanisms until
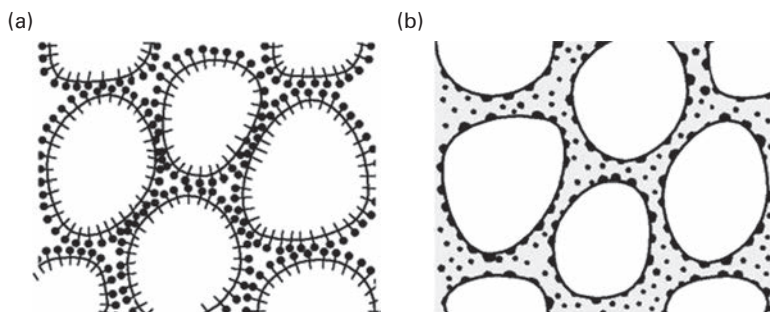
**Fig. 8.1**　(a) Bubbles stabilized by chemical surfactant consisting of a two-phase (gas–liquid) system and (b) bubbles stabilized by particles consisting of a three-phase (gas–liquid–solid) system. The bubble, chemical surfactant and particle sizes are not comparable. The particle-stabilized bubbles are about ten times larger in size. From ref (1).

recent years; today a considerable amount of insight has been achieved in understanding the basics.

Developments in the production of commercial particle-stabilized foam systems were mainly driven by the fact that particles could have several economic and environmental advantages compared to traditional surfactants. For example, improvement in performance may be achieved and also the potential use of less organic chemicals is attractive. Although most studies have been focused on stabilizing foams with partially hydrophobic particles, it is also important to note that non-adsorbing particles (hydrophilic) can also act as foam stabilizers through "stratification" (or stepwise film thinning). This is less commonly encountered and usually involves spherical monodispersed particles which are forced into ordered layers. As they are expelled out of the thin lamellar foam films in a stepwise manner, they enter the Plateau borders and reduce drainage, as discussed earlier in Chapter 7.

A considerable amount of work has been focused on determining the conditions needed for foam stability in terms of critical hydrophobicity, size and shape of the particle or the critical bubble size or water content of the foam or the capillary pressure. This work was reviewed in some detail by Hunter and coworkers (4), and from the literature it is possible to establish some general rules which act to guide foam stability in the presence of particles. In general, it has been established that foam stabilization can be successfully achieved if a high concentration of small (nano-sized) particles of moderate hydrophobicity (contact angle about 60 to 70°) is used. However, de-stabilization may result with the use of a lower concentration of larger particles of high hydrophobicity. Partial coagulation of particle networks (produced from nano-sized particles) has been found to be advantageous for stability, especially if they have low to moderate contact angles. In conclusion, it is generally accepted that the mechanisms are complex, but overall the concepts of particles creating steric barriers to prevent bubble coalescence were validated. It also appears that one of the unique features of particles in foam systems is that they can cause blockage of the three-phase regions between films, and within the Plateau borders which leads to a reduction in or prevents drainage. There is evidence that weak flocculation or gelling of a film of particles can improve stability, and if a closely packed coagula or gel is deposited

on the particles, then it may be sufficient to provide a high elastic modulus to prevent shrinkage during disproportion. However, the role of salt coagulants may complicate this deposition process by changing the particle contact angle, and specific ion effects can also have an influence on the process (5).

## 8.2 History of particle-stabilized foam systems

Pioneering work carried out in the early part of the 20th century was mostly focused on the flotation of mineral ores and has been well documented. In 1913, Hoffmann indicated that finely divided particles played a role in the stabilization of foams or froth (6). Later, in 1925, Bartsch reported that partially hydrophobic particles stabilized froths, but completely hydrophilic (wetted) particles had no effect on foam stability (7). Later, Hausen (8) found stabilized three-phase froths could be generated with various metal oxide and clay particles. Ottewill (9) reported an increase in foam stability with dispersions of alkali metal carbonates that he attributed to the increase in bulk viscosity of the dispersion. During the past 20 years there has been an intense interest in the use of nanoparticles to stabilize foam systems. For example, Blute and coworkers (10) showed that commercially manufactured partially hydrophobic silica nanoparticles enhanced the stability of foams in deionized water. More commercial-orientated projects have been directed toward using more environmentally friendly particles such as cellulose fibers or cellulose microparticles to stabilize foams (11, 12).

## 8.3 Established processes

The froth flotation process highlighted the practical importance of producing stable froths in the presence of partially hydrophobic, non-spherical, fairly dense particles. This process is widely used as a separation method for mineral particles dispersed in a liquid pulp and involves the capture and the attachment of particles to bubbles which ascend to the surface, where the particles are then collected. The bubble/particle aggregates play a critical influence on the stability of the foam. In the industrial process, it is generally known that it is the finely dispersed partially hydrophobic particles together with a weak chemical foaming or frothing agent that adsorbed at the bubble interface and enhanced the stability of the bubbles. These wet flotation froth systems show differences in structure compared to a well-drained (dry) detergent foam, and in Fig. 8.2, a froth stabilized with galena particles (PbS) is shown as a comparison.

Achieving high separation and recovery of the valuable mineral components in the froth flotation process for sulfide minerals also requires a delicate balance between the type and concentration of the chemical collector (usually a xanthate compound) and the type and concentration of the frother (usually a weak non-ionic molecule such as a low molecular weight aromatic alcohol or a branched chain aliphatic alcohol). However, the size range, density and shape of mineral particles in the many different types of flotation processes vary considerably.
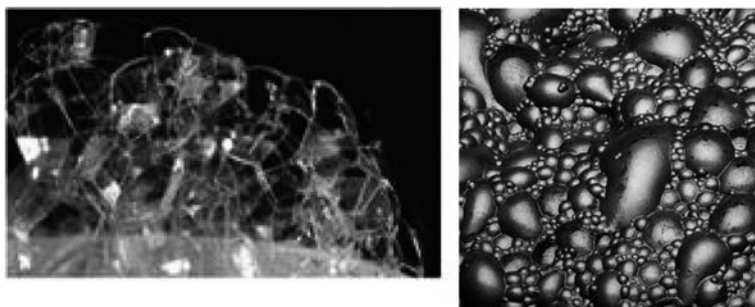
**Fig. 8.2**        Comparison of a detergent foam and a flotation foam heavily loaded and stabilized with galena particles. Bubbles are in the mm to cm size range in both cases.

Knowledge of the particle stabilization process is also especially important for deinking flotation where a great range of different types of ink particles are encountered. These are mostly in the smaller size range (< 1 micron) and are known to play an important role in stabilizing the bubbles. In Europe, long-chain fatty acids in the presence of calcium ions are "the chemical workhorse" of the hot deinking process and cause agglomeration of the ink particles (2). This leads to the formation of relatively large hydrophobic agglomerates which can be fairly easily removed by the stream of air bubbles that ascend to the surface of the flotation cell, leaving the fibers dispersed in the bulk liquid. The bubbles with the attached hydrophobic particles are carried to the froth and rupture, yielding ink removal and minimal fiber loss. In general, this process has proved to be highly selective and economical. It is well known that the fatty acid renders the ink particles hydrophobic but the mechanism has been under dispute for several years. One mechanism suggests that $Ca^{2+}$ ions induce a direct bridging mechanism with the anionic fatty acid species. It has also been suggested that the $Ca^{2+}$ ions interact with the negatively charged surface groups on the oil-based ink particles. The adsorbed $Ca^{2+}$ ions would reduce the negative charge and could lead to a carboxylic acid bridging mechanism with the $Ca^{2+}$ ions, specifically adsorbing to the negatively charged sites on the ink particles. There is also the possibility of build-up of calcium soap particles around the ink particles (microencapsulation) through hetero-coagulation of bulk precipitated calcium soap fatty acid particles. These mechanisms are outlined in Fig. 8.3.

Using the surface force apparatus, Rutland and Pugh (13) have studied the interaction of a fatty acid collector with $Ca^{2+}$ ions in water using a negatively charged mica surface to simulate the ink particle surface. From this fundamental study, no evidence of $Ca^{2+}$ ion bridging was detected, but a $Ca^{2+}$ ion dehydration destabilization was detected at low concentrations of fatty acid below the calcium soap solubility limit, where calcium ions adsorb on the ink particles and lower the surface charge. At high fatty acid and calcium soap concentrations, calcium soap was precipitated in bulk solution. Overall, it was concluded that the main mechanism involves insoluble calcium soap formation, and this becomes associated with the detached printing ink particles. The bubbles capture the aggregates and rise to the surface, and the printing ink particles are skimmed off as froth. An enhanced understanding of the behavior of ink and fiber particles in the froth phase can lead to an increase in recovery and an overall improvement in recycling yield.
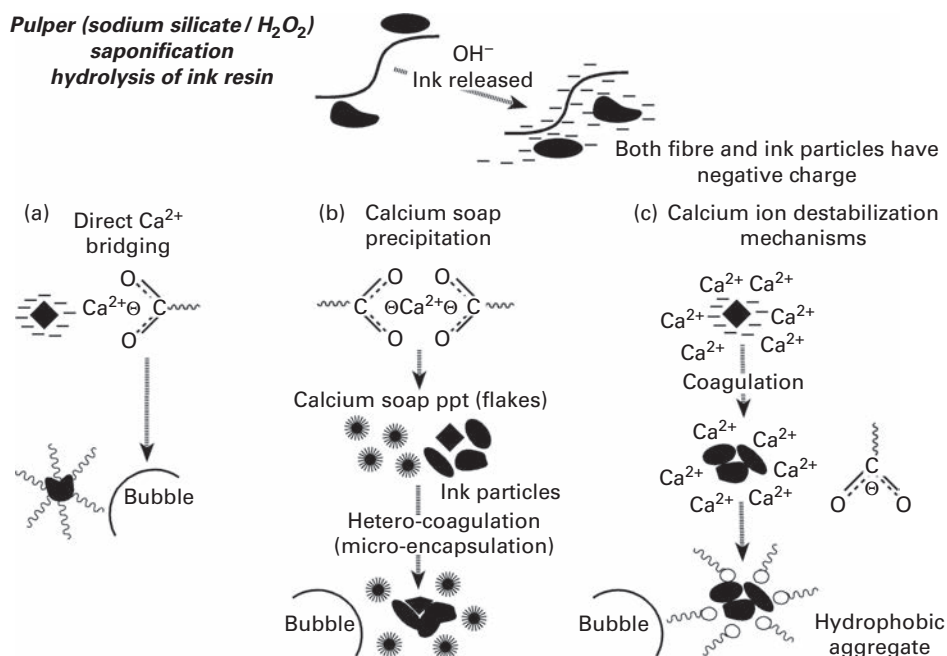
**Fig. 8.3** Possible mechanisms involved in calcium soap deinking. From ref (13).

It is also well known in the food industry that adsorbed particles influence the texture and long-term stability of foams (3). These are in the form of networks of solid fat crystals which adhere to the bubble surfaces. Traditional products such as bread and beer contain foam structures. In addition, in the dairy industry, during the whipping of cream partially crystalline "solid" oil droplets accumulate at the interface and stabilize the foam. Particles are also used in the fabrication of cellular material and metal foams, and there has also been some effort to develop various kinds of novel engineering products based on particle-stabilized foams. However, particles are known to have a negative impact on some industrial processes; for example, foaming occurs during the agitation of radioactive wastes. In the paper industry, the dispersion of sludge and pulping is caused by particles and this can delay production. In the oil industry, obnoxious foams, produced in boilers and at various stages of distillation, are thought to be stabilized by asphaltene particles. In other cases, heterogeneous nucleation of insoluble precipitates (hydrolyzed cations such as iron hydroxides) at the air/water surface can also cause foaming in waste water or rivers.

## 8.4 Fundamentals of collision, contact angles, attachment/detachment

To achieve stability, it is essential that particles attach to the bubbles and eventually build up a skin of particles. This process occurs through collision and retention, which have been considered separately, and involves other sub-processes such as impaction, attachment and detachment. The background to these processes has been earlier documented
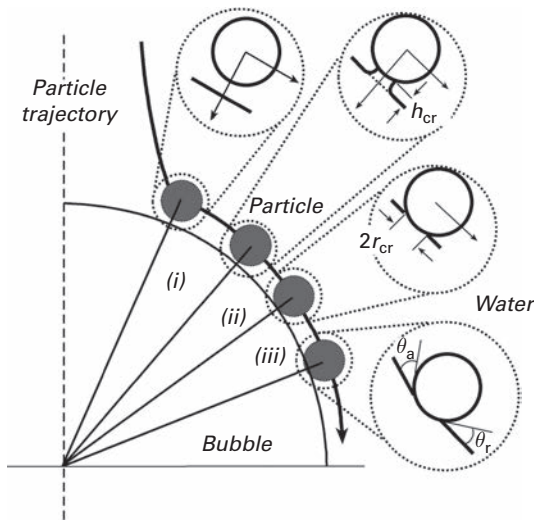
**Fig. 8.4**      Bubble–particle attachment steps: (i) thinning of the intervening liquid film to a critical thickness $h_{cr}$, (ii) rupture of the intervening liquid film formed when the bubble and the particles are close together and the formation of the three-phase contact nucleus with radius $r_{cr}$ and (iii) spreading of the TPCL from the critical radius to form a stable wetting perimeter with equilibrium contact angles (advancing $\theta_a$ and receding $\theta_r$). From ref (1).

in considerable detail by Schultz (14), and advances in this area have been reviewed by Nguyen and coworkers (1). In these theories, both the physical properties of the particle and bubble and the hydrodynamics of liquid flow are taken into consideration, and several different models have been developed to explain the experimental results. The modeling of these processes is complex and involves hydrophobic interactions and de-wetting hysteresis, and the influence of the chemical heterogeneity of the particles surface also has been taken into consideration. Attachment of the particle to the bubble involves the initial thinning of the thin liquid lamellae in which the interfacial forces define the stability. Following rupture of the film, a three-phase contact line (TPCL) becomes established; this spreads across the solid surface at a specific rate to form a stable wetting perimeter. The various steps leading to bubble/particle attachment are shown in Fig. 8. 4.

The total time required for the bubble attachment process ($t_{att}$) has been defined in terms of the sum of the times of several individual processes and is expressed as

$$t_{att} = t_i + t_r + t_{tpc} \qquad (8.1)$$

where $t_i$ is the induction time, which is the time required for the film to reach a critical thickness, $t_r$ is the time for film rupture and for the formation of the three-phase contact nucleus and $t_{tpc}$ is the time for the TPCL to expand from the radius of the nucleus to establish a stable wetting perimeter. Under normal circumstances $t_r$ is of the order of 1 ms, which is shorter than $t_i$ and $t_{tpc}$. Many studies have focused on the physics of modeling and measurement and contact times and the spreading rates.
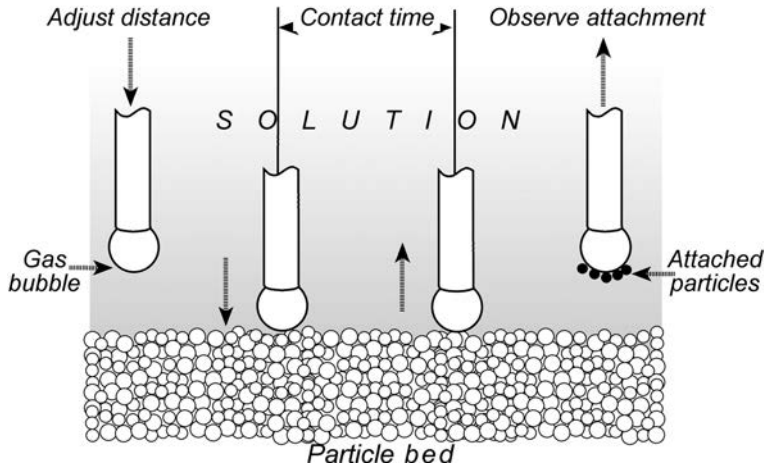
**Fig. 8.5**     Measurements of the attachment time using a particle bed. From ref (1).

## 8.5     Measurement of attachment time between bubble and particle

The value of $t_{att}$ is important since it gives an indication of the process kinetics and can be measured by using the equipment shown in Fig. 8.5. The procedure is relatively easy and was originally developed in the area of flotation research. Initially, a fresh captive bubble of known size is produced in a glass capillary tube and pressed downward through the solution in a cell so that the tip of the bubble makes contact with the bed of particles. It is then retained in this position for a predefined time period. This is known as the contact time. The bubble is then released from the bed and returned back to the original position above the bed. It is then observed through the microscope to determine if particles have become attached to the bubble during this contact time. Experiments are repeated, with the bubble making contact with different points on the bed so that an average result can be obtained. The contact time is then extended and the procedure repeated. The number of successful attachments is plotted against the contact time and the attachment at the minimum possible contact time, is determined. The value of $t_{att}$ is then usually estimated as that specific contact time at which 50% of the observation results in the successful attachment of particles to the bubbles. From further experiments the influence of the attachment time on particle size and also the influence of pH and surfactant concentration can be studied. In flotation systems, the highest flotation recovery corresponds to the shortest attachment time.

## 8.6     Relationship between attachment force and contact angle

Following the contact of a spherical particle with a bubble, three situations can be considered, as illustrated in Fig. 8.6 (a, b and c).
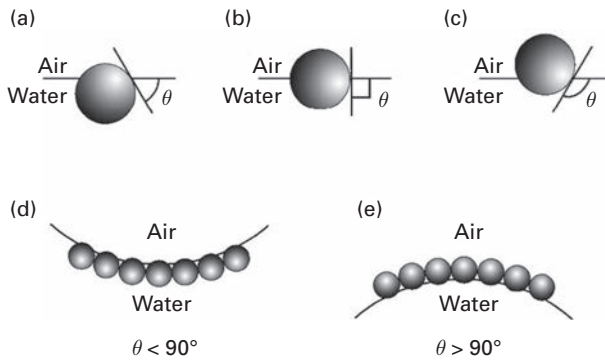
**Fig. 8.6**     (a, b and c) The location of an individual particle at air/water interface where the contact angle is measured through the water. Particles are anchored when (a) $\theta < 90^{\circ}$ and when (b) $\theta = 90^{\circ}$. In (c) the hydrophobic solids are characterized with $\theta > 90^{\circ}$ and reside on the air side of the interface. In (d and e) monolayers of particles are shown which determine the curvature of the interface.
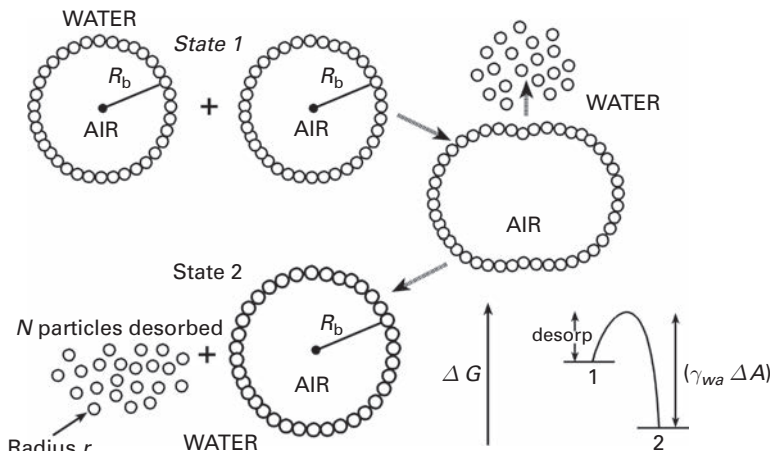


**Fig. 8.7**     Coalescence of two bubbles that are covered with particles. The adsorbed particle must be removed from the interface, which requires an energy barrier to be exceeded. From ref (15).

Theoretically it is the magnitude of the contact angle $\theta$ (measured through the aqueous phase) which defines the position of the particle with respect to the interface, as indicated in Fig. 8.6. Fig. 8.6(a) illustrates a wetted particle ($\theta < 90^{\circ}$) with a high immersion depth, whereas Fig. 8.6(b) shows a partially wetted particle with an intermediate immersion depth ($\theta$ about $90^{\circ}$) and, finally, Fig. 8.7 (c) shows a non-wetted particle with a low immersion depth ($\theta > 90°$). For a packed monolayer of particles attached to the interface, it is the contact angle of the particles (hydrophobic/hydrophilic balance) that determines the curvature. For $\theta$ of $90°$ (partially hydrophobic particles), a large fraction will reside

on the water side of the interface, but in the case of $\theta > 90°$ (strongly hydrophobic particles) a large part of the area will reside in the gas phase. Strongly hydrophobic particles are ineffective as foam stabilizers and will break the foam upon opposing bending energies. Generally, the terms hydrophilic and hydrophobic refer to particles of contact angles ($\theta < 90°$ and $\theta > 90°$) respectively, but usually particles with contact angles of less than 70° are used to stabilize foams. A further aspect of particle wettability is that it parallels the hydrophile/lipophile balance (HLB), as discussed in Chapter 2. The hydrophobicity of the particles can also be increased by screening or reducing the surface charge on the particles, and charged particles are usually hydrophilic. In order to relate $\theta$ to the surface tensions of the particle/air, particle/water and particle air/water, an equilibrium situation is assumed, and the forces per unit length parallel to the solid surface at the junction of the three phases can be resolved by applying Young's equation

$$\cos \theta \ = \ (\gamma_{pa} - \gamma_{pw})/\gamma_{aw} \tag{8.2}$$

where $\gamma_{pa}$, $\gamma_{pw}$ and $\gamma_{aw}$ are the particle/air, particle/water and particle air/water surface energies, respectively.

## 8.7 Detachment of particles from bubbles

To ensure foam stability, it is important that the particles remain attached to the interface to prevent the coalescence of bubbles. For coalescence of coated bubbles to occur, the total interfacial area needs to be reduced and particles must be ejected. One of the keys to retaining stability is hence the magnitude of the detachment force, and theoretically in the case of bubbles with densely compact monolayer coatings, a high energy is required to reduce the area and expel the particles. If the free energy associated with desorption is larger than the free energy decrease caused by reduction of surface area, the coalescence will not be spontaneous. Fig. 8.7 shows how an energy barrier needs to be overcome to expel a fraction of the particles from the interface.

Based on this thermodynamic approach it can be shown that the decrease in free energy associated with this process is critically dependent on the size of the particle and the contact angle. The analysis of the process for a single spherical bubble attached to a flat interface has been documented by Lopetinsky and coworkers (15). Assuming the buoyancy/gravity effects are not taken into consideration, the decrease in energy can be expressed by the equation

$$\Delta G_{ads} = \Pi r_b^2 \gamma \ (1 \pm \cos\theta)^2 \tag{8.3}$$

where $\Delta G_{ads}$ is the adsorption energy in joules, $\gamma$ is the gas/liquid interfacial tension (N/m) and $r_b$ is the particle radius (m). In the case of $0° \leq \theta \leq 90°$ the positive sign is used, whereas the negative sign applies when $> 90°$. According to this equation, the maximum in free energy corresponds to the contact angle of 90°, but the energy falls off sharply as

the angle and particle size are reduced. A simple calculation shows that for relatively small particles, the adsorption energy of the particles can be several thousand times $kT$. For example, for a particle of diameter 10 nm, the maximum energy to detach the particle (90°) would be about 1400 $kT$, but for a contact angle of 13° it would be only about 1 $kT$. Based on this relatively simplified fundamental approach, the value of the parameter $\theta$ is the single most important indicator that determines the feasibility of a spherical particle remaining attached to the interface, and a contact angle close to 90° suggests the particle can become almost irreversibly absorbed.

In order to predict the effectiveness of particles to stabilize foams, it is important to obtain an accurate value of $\theta$ to calculate the energies of detachment. However, this is difficult to achieve especially for nanoparticles, although for micron-sized particles the contact angle of a water drop in air on a pressed tablet prepared from micron-sized particles has frequently been used to estimate a value. Another problem in relating $\theta$ to stability is hysteresis, since the attached particles are irregular in shape and rarely attach as a monolayer coating. In earlier papers, it was found that several other parameters, in addition to $\theta$, have an important influence on the behavior of particles at the air/water interface. These include the shape and degree of agglomeration of the particles. In real systems, particles are rarely spherical or smooth and are often elongated with spikes which can pierce the surface, causing rupturing of the foam films separating the bubbles, which are extremely delicate. Hence, under practical conditions contact angles for maximum stability are considerably to be less than 90$^o$ and regularly in the region of 60–70°. However, the situation is further complicated by the dynamic conditions which occur during the generation of bubbles during whipping, where the local dynamic interfacial properties will also influence the detachment process. It is therefore almost impossible to make an accurate assessment of the attachment energies, and the thermo-dynamic model can only be generally used in a qualitative sense.

## 8.8        Surface tension of films of attached particles

Although surface tension is a critical factor in defining the surface-active nature of particles, there have only been a limited number of comprehensive studies reported. In the case of industrial manufactured silica nanoparticle sols dispersed in ionized water, only slight reductions in surface tension were observed, and the differences between the hydrophilic and partially modified hydrophobic (by chemical silane treatment) nano-sized particle sols were small (16). In Fig. 8.8, the surface tension versus concentration data are shown for three different types of nanoparticle systems dispersed in weak electrolyte at different pH values. These results indicate that the hydrophobic modified sols (designated Bindzil CC30) are more surface active at the higher concentration range than the hydrophilic sols (designated Bindzil 30/360FG and Nyacol 2034DI). The hydrophobically modified sols also show greater surface tension/concentration gradient and were also more pH responsive. For this system, the greatest reduction in surface tension was found to occur at low pH (in the region
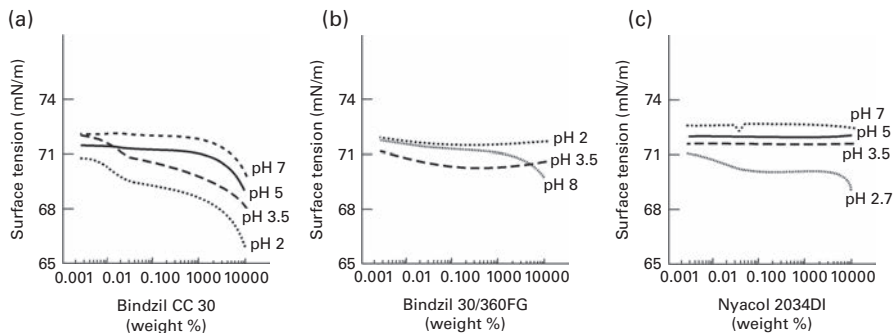
**Fig. 8.8** Surface tension versus concentration of dispersions of silica nanoparticles in 0.01 M NaCl at different pH values (a) hydrophobic modified Bindzil CC30 with a $pH_{pzc}$ value of <1.5 and (b) hydrophilic Bindzil 30/360FG with a $pH_{pzc}$ value of 4. (c) Nyacol 2034DI with a $pH_{pzc}$ value of <1.5. The silica nanoparticles were manufactured by AkzoNobel, Sweden. From ref (16).
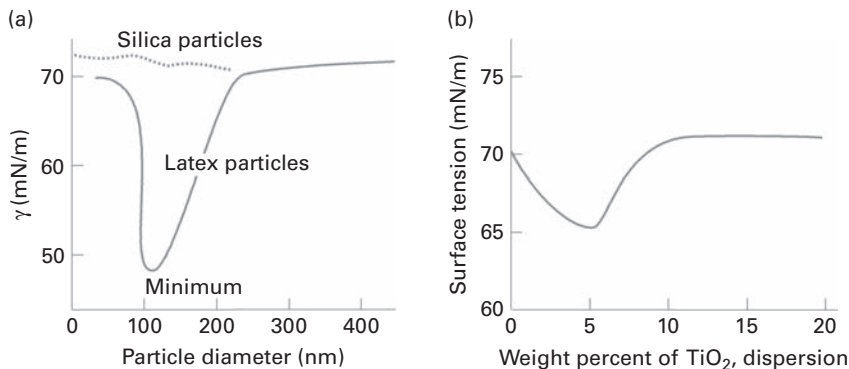


**Fig. 8.9** Surface tension versus particle size of (a) silica and latex (mass fraction 0.2 w%). From ref (17). (b) Surface tension versus concentration for $TiO_2$ particle suspension at pH 11–12. From ref (18).

of the $pH_{pzc}$) where the charge was in the minimum range, and this correlated with the highest foamability.

Okubo (17) also used surface tension measurements to study the distribution and ordering of colloidal spheres at the air/water interface. Experiments were carried out in deionized water with two kinds of colloidal systems: monodispersed hydrophobic polystyrene latex particles and hydrophilic silica particles. In Fig. 8.9(a) the relationship between the surface tension and particle size plot is shown for both the silica and hydrophobic polystyrene spheres. In the case of the colloidal silica (size ranges 10 to 200 nm) only a relatively minor reduction in surface tension occurred, suggesting very weak surface activity. On the other hand, with polystyrene spheres, the surface activity was unusually high for spheres of a particular critical size range diameter (from 100 to 200 nm). In fact, the surface tension reduction passed through a sharp minimum for particle diameters of approximately 100 nm. A value of about 20 mN/m below that of water at relatively high particle concentrations (10–20%) was observed. The reductions

in surface tension were explained by the structural ordering of the particles, and crystal-like, liquid-like and gas-like structures in both the bulk solution and at the interface were suggested. This relationship between particle size and surface activity for the hydrophobic particles would appear to be a significant finding.

Surface tension measurements on charged stabilized hydrophilic $TiO_2$ dispersions were studied by Dong and Johnson (18). The influence of the bulk particle concentrations on surface tension is shown in Fig. 8.9(b). The surface tension was found to initially decrease at increasing concentrations, reaching a minimum at around 5–7% solids, before rising back to a value about the same as water. It was suggested that as the concentration of particles at the interface was initially increased, the free energy of the system decreased as expected; but at higher particle concentrations, capillary force, which acted as a resistance to interfacial deformation and effectively increases the local effective surface tension becomes significant.

These reports highlight the complexity involved in the relationship between surface tension fluctuations and interactions of the particles in the interfacial region. Reduction in surface tension has also been explained by partial crystallization and the aggregation of particles within certain size ranges. The role of capillary attraction in modifying the surface energy may also be an important regulating factor. Carlson and Johnson (19) gave support to the idea that capillary forces had an important influence on surface tension from studies carried out with latex particles which were spread on the air/water interface in an open dish. Initially, random aggregation was observed, causing a build-up of coagula, and this process appeared to be associated with fluctuations in the local surface tension, possibly caused by particle flow.

## 8.9     Interactions between neighboring particles attached to the interface

Several different types of interactions can occur between small particles attached to the interface, and these can influence the packing density, contact angle and the magnitude of the attachment forces. Dong and Johnson (18) used a simplified approach to classify the configuration of attached particles into different categories: flotation, where the particles are freely floating as indicated in Fig. 8.10(a); or partially immersed (confined)
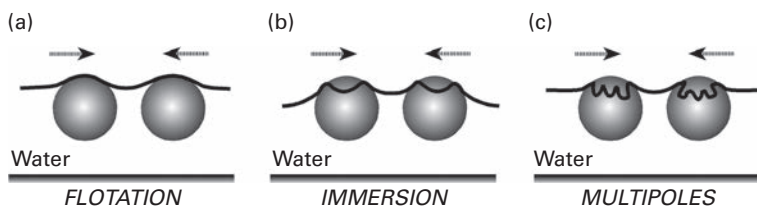


(a)                    (b)                    (c)

Water                  Water                  Water

*FLOTATION*            *IMMERSION*            *MULTIPOLES*

**Fig. 8.10**     Two particles at an interface: (a) freely floating particle, where origin of force is particle weight, and (b) a partially immersed particle confined into a liquid layer. The origin of capillary force is the wetting of the particle by the liquid. (c) If contact line on the particle surface is irregular a multipole–multipole capillary force exists between particles. From ref (17).

particle, where the particle is immersed into the liquid layer with a regular interface (Fig. 8.10(b)) or is confined with an irregular meniscus, as indicated in Fig. 8.10(c). The importance of the irregular meniscus in a capillary interaction for small immersed particles was discussed by Levine and coworkers (20).

In the case of flotation, the gravitational force acting on relatively large particles (> 10 microns) can cause direct deformation of the interface and the magnitude of the interaction between attached particles is dependent on particle size and density. However, for particles below 10 $\mu$m, gravitational effects are negligible but capillary forces act laterally between close particles. For the immersed particles, the attraction is related to the wetting properties of the particle surface, the particle size, shape and the overlap of menisci. The general interaction of small particles caused by capillary attraction was discussed by Kralchevsky and coworkers (21, 22) in terms of the immersion in the liquid phase which causes meniscus deformations. The capillary attraction results from restricted surface wetting. In the case of an irregular meniscus, Lucassen (23) developed a model taking into account the influence of the capillary pressure caused by sinusoidal-edge disturbances (undulated contact line), and it was shown that this could cause a significant interaction between neighboring particles. Both dipole–dipole interactions between particles, as first proposed by Pieranski (24), can also occur through the polar phase, (aqueous phase), resulting from the asymmetrical distribution of charges as the particle surfaces become ionized. For particles with ionizable surface groups such as latex or silica, parts of the particles immersed in the aqueous phase will become charged, creating asymmetric charge distributions on the particles and dipoles perpendicular to the interface.

In addition to capillary forces, dipole–dipole interactions and particle–particle electrostatic double-layer repulsive forces can operate between particles attached to the interface through the aqueous phase. Van der Waals attractive forces, which operate through both the aqueous and the air phases, also need to be considered. The effects of surface change and salt counterions can play a role, and this may lead to decreased attraction and may cause interfacial coagulation. Based on a theoretical approach, Levine (20) concluded that the double-layer repulsion was the most significant repulsive force, and dipole–dipole repulsive energies were relatively small (in the range of ~0.8 kT). Dipole–dipole repulsion is significant in systems where particles contain strongly ionizable surface groups in a medium of low dielectric constant (i.e. air). Fernandez and coworkers (25) summarized these different types of interactions (excluding capillary forces), as shown in Fig. 8.11.

Since charge neutralization is dependent on the degree of aqueous immersion, more hydrophobic particles will attain stronger dipole–dipole interactions. However, from experimental studies it proved extremely difficult to firmly establish which forces play the most important role in real systems, and there has been some conjecture on the importance of dipole–dipole repulsion forces in air–water systems. Experimental studies by Abdel-Fattah (26) and Williams and Berg (27) questioned the magnitude of dipole–dipole forces on particle adsorption at air/water interfaces. Both found that at moderately low salt concentrations, extensive particle aggregation on the surface, occurred at concentration levels up to two orders of magnitude below bulk conditions.
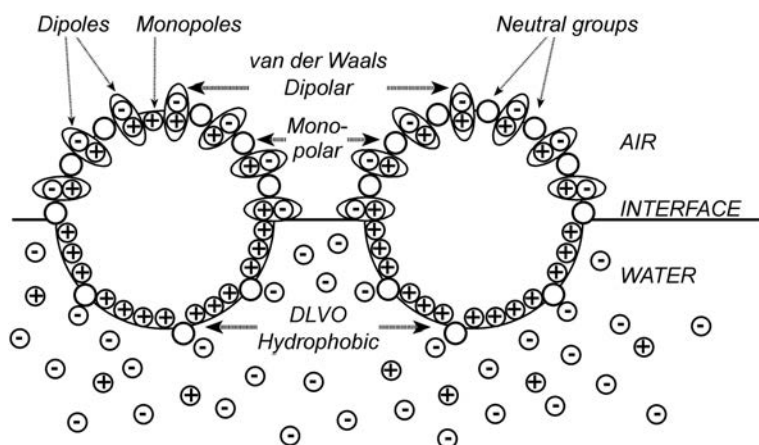
**Fig. 8.11**    Two particles located at the air/water interface. The immersed parts of the particle interact through DLVO and hydrophobic interactions and the emergent parts interact through Van der Waals, dipole and monopolar interactions. From ref (25).

These conditions were considerably below that anticipated if significant dipole–dipole repulsions were present.

Several experimental studies have also been carried out in an attempt to determine the influence of these interactions on the state of agglomeration of the particles. It was found that different types of interactions can lead to the formation of 3D aggregation and networks in the interface. For example, experimental studies by Aveyard and coworkers (28) also found unexpected aggregation of particles at air–water surfaces, but, especially in this case, particle–water contact angles were very low. Robinson and Earnshaw (29) showed that decreasing particle contact angles (rendering particles more hydrophilic) caused the dipole–dipole forces to be reduced in line with increased counterion screening, and the aggregation too was increased. Ghezzi, Earnshaw and coworkers (30) further showed that by applying charge to the interface, aggregation was induced by retarding the dipoles through counterion screening in the air phase. These workers also found that under certain conditions, particles aggregated into complex chain and meso-structures. This was explained by a secondary energy minimum coagulation process (attraction force) at long-range distances (beyond the possible range of Van der Waals attraction).

In general, the Langmuir Blodgett (LB) technique proved to be a useful method to monitor changes in the state of aggregation of nanosized particles at the air/water interface. Blute and coworkers (31) used dispersions of hydrophilic and partially hydrophobically modified, industrially manufactured silica nanoparticles. The commercial silica sols were manufactured and supplied by Eka Chemicals, AB, Sweden. They were produced from sodium silicate using a cation exchange process that produced silicic acid, which was then polymerized under controlled conditions. The hydrophobic modified sol (designated Bindzil CC 30) was produced by converting some of the sinanol surface groups to alkoxy groups by an esterification process. The results of these studies are shown in Fig. 8.12. The hydrophilic particles featured expanded, fairly
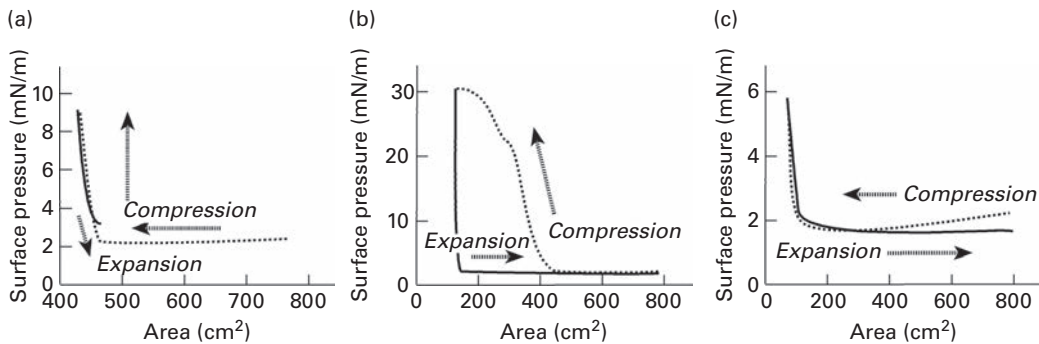
**Fig. 8.12** Surface pressure (p)–area (A) isotherms obtained by compression of films of silica particles. (a) The compression/expansion before collapse point of a hydrophilic sol (Nyacol 2034DI particle size 20 nm) supplied by Eka Chemicals AB, Sweden. (b) Compression/expansion of the hydrophilic sol (Nyacol 2034DI) over the whole trough area. (c) Compression and expansion of hydrophobically modified silica particles (Bindzil CC30, particle size 7 nm) spread on 0.01 M NaCl at natural pH. A mixture of chloroform and ethanol (50/50 vol/vol%) was used as the spreading solvent. From ref (31).

easily compressible, surface pressure ($\pi$)–area (A) isotherms with well-defined collapse pressures that appeared to be caused by the formation of loosely structured agglomerates that exhibited elastic behavior at low surface pressure and inelastic behavior at high surface pressure. Lateral electrostatic interparticle interactions seemingly played an important role in this hydrophilic system. This contrasted with the hydrophobically modified particles, which were more difficult to disperse in the ethanol/chloroform spreading solvent, appeared to be in the semi-agglomerated state at low surface pressures and exhibited a more difficult-to-compress compacted film. Both types of particulate films were shown to be sensitive to the spreading environment, and changes in pH were found to increase particle agglomeration; this drastically reduced the particulate area for the hydrophilic particles but less so in the case of the moderately hydrophobically modified particles. These results also appear to give some support to the idea that particles can produce an aggregated particulate film surrounding the air/water interface, which provides a physical barrier preventing coalescence of bubbles.

## 8.10 Key parameters influencing the interactions between bubbles and particles

Although steric forces play a primary role in regulating the interaction between bubbles coated with particles, other parameters such as particle size, roughness, contact angle, density and extent of particle aggregation may be considered to play a secondary role. From experimental stability studies, it can be concluded that particle-stabilized foam systems are under a number of critical constraints. In fact, it has been proposed that the stability "window" for particles in terms of size and contact angle is relatively small. In terms of foam stability performance, probably the most pressing issue is therefore to

increase the range (in effect of stability "window") of particle effectiveness. However, at present it is difficult to formulate rules that could lead to an improvement in the performance of specific systems. This is an important area for future research. At present most experimental studies have been carried out with different types of particles in an attempt to develop super-stabilized foams, but these have been mainly based on trial-and-error methods.

## 8.11    Steric barriers

In addition to size, the shape of the particles also needs to be considered with regard to these interactions. Fig. 8.13 shows schematically the interactions between differently shaped particles with different sizes. In Fig. 8.13(a) and (b) spherical and irregular particles are considered, whereas in Fig. 8.13(c) the orientation of the rods probably determines whether they pierce the liquid film causing coalescence or act as a steric barrier to protect the bubbles. When one considers the complexities, it is not therefore altogether surprising that a theoretical understanding of the interactions between irregularly shaped particles attached to interface has not been achieved. Single layers of particles can act as effective steric barriers and also reduce drainage, and the lateral movement of particles along the contact interface needs to be taken into consideration, as well as the possibilities of expulsion of particles into the liquid during film thinning.

The importance of the film curvature relative to the size of particles on the foam stability was demonstrated by Alargova and coworkers (32) using small flexible plastic rods. In their study they prepared highly anisotropic micro-rods produced from epoxy resin (average length 23 microns and diameter 0.6 microns with a contact angle about 8°). The rods were reported to be effective foam stabilizers, and foams that were stable for weeks were generated with low concentration (0.2 to 2.2 wt%). The rods appeared bent and entangled around the bubbles as a wool-ball or dense thick hairy layers and appeared to give some degree of steric protection. This study clearly showed that rod curvature, rod length and rod rigidity were important in foaming. Foaming experiments with rod-shaped particles were also carried out by Zhou and coworkers (33), but in this case rigid hydrophilic calcium carbonate rods (20–80 micron length and 0.5 to 1 µm diameter)
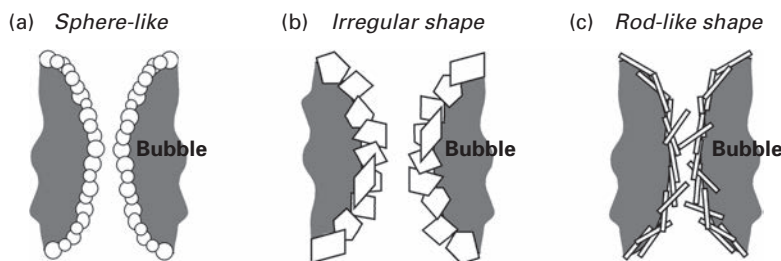


(a) *Sphere-like*    (b) *Irregular shape*    (c) *Rod-like shape*

**Fig. 8.13**    The effect of particle morphology on coverage. (a) Uniform coverage with small sphere like droplets; (b) large irregular particles producing irregular overage; (c) rod like particles which are physically entangled causing bridging and piercing the thin foam film, leading to coalescence.

were used in the study. The surfaces were hydrophobized (by chemical treatment with oleic acid), and the partially hydrophobic rods appeared to coat the bubbles with an armored microstructural domain in a tangential direction to the curvature. In this case, the structures appeared to differ from the flexible epoxy rods, which were found to bend around bubbles. In fact, it appeared that these self-assembles of calcium carbonate rods preserved their shape on the bubbles, with the rod length having a size comparable to the bubble curvature. In Fig. 8.14, the microstructures are shown for several different-sized bubbles. The surface patterns observed appeared to be similar to the structures formed on the surface by large logs when transported by rivers.

Super-stabilized bubbles were generated using these rods, and they did not collapse during drying. It was suggested that the diffusive disproportionation was reduced due to blockage caused by the adsorbed rod layers at the bubble surface rather than
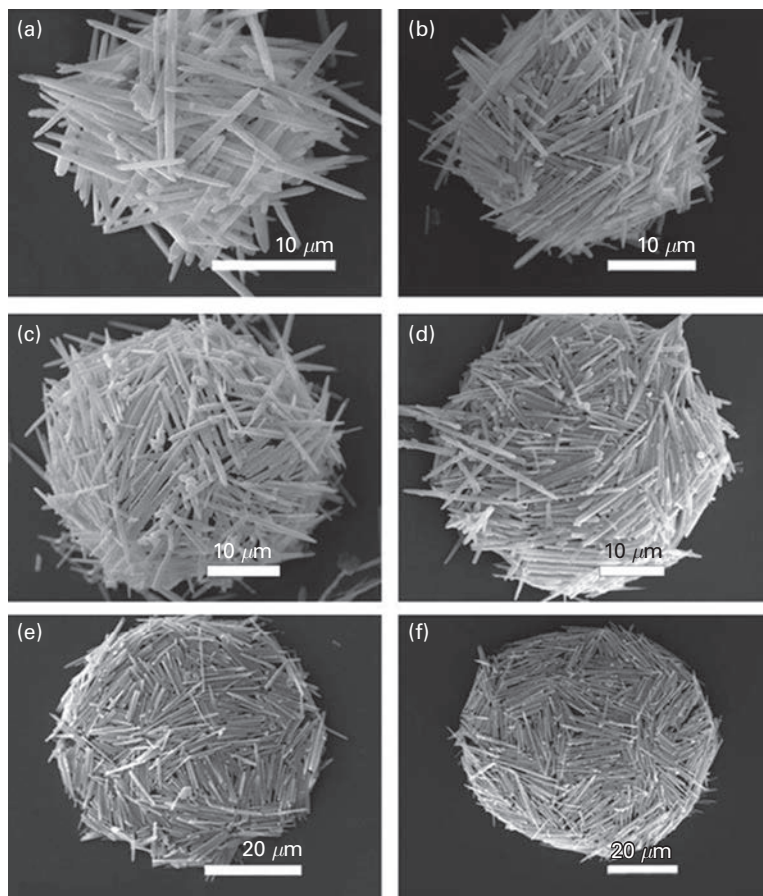


**Fig. 8.14**   Microstructure evolution of bubble stabilized by $CaCO_3$ rods. (a) 20 μm rods; nestlike microstructures with rods tangent to the bubble surface. (b) and (c) 30 μm and 40 μm bubbles; transition microstructure with overlapped rods and semi-ordered domains; and (d), (e), and (f) 50, 60 and 80 μm bubbles armored microstructures with ordered domains constructed by oriented rods, especially for the 80 micron bubbles. From ref (33).
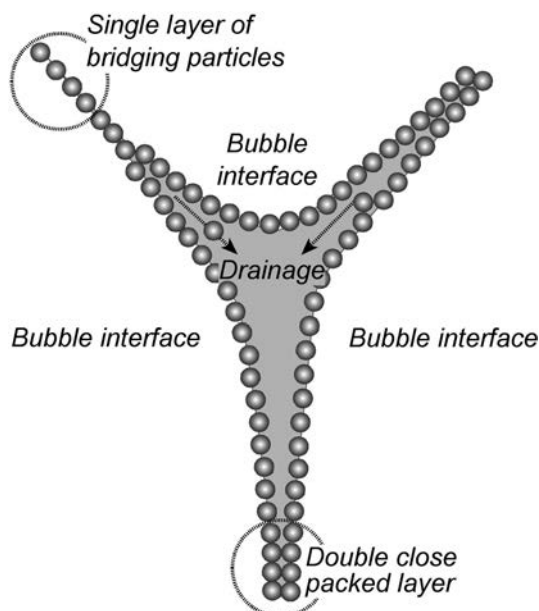
**Fig. 8.15**        Stabilization of polyhedral foams by a zipping mechanism. From ref (4).

solidification or gelling of the continuous phase or in the structural nodes. An alternative mechanism has also been suggested to explain the stability of dry foams generated by monolayers of spherical particles attached to the interface. This involves bridging of particles during the final stages of thinning, causing a high force contact area which could be important in the stabilization of polyhedral-type structures. Since the particle movement in the bridge would be greatly impeded, eviction of particles may occur, causing a kinetic zipper-like closure at the lower boundary of the thin film region. The magnitude of the contact angle would play a critical role in this type of mechanism, which is illustrated schematically in Fig. 8.15.

Experimental studies have also led to a debate concerning the actual state of aggregation of the particles on the stability of the foam. In fact, there has been some evidence that high stability only occurs in the presence of weakly flocculated or gelled films of particles. However, it has not yet been established whether gelation or high elastic surface modulus acts as a resistance to collapse during the shrinkage of bubbles during gas diffusion.

## 8.12        Experimental studies relating contact angle and wetting on particle attachment and stability

Although it is generally accepted that particles with contact angles below 90° can act to some extent as foam stabilizers, many experiments have indicated that particles with high contact angle values can also act as foam breakers. For example, Pugh and Johansson (34) considered the effects of the hydrophobicity of quartz particles in

regard to mineral processing. They found particles with $\theta < 40°$ gave no effect, whereas particles with a contact angle around 65° gave optimum froth stability. More hydrophobic particles with contact angles still below 90° caused the froth to collapse. Schwarz and Grano (35) found similarly that optimum particle contact angles for stability occurred around 63°, and Ata and coworkers (36) in experiments using froth flotation columns to selectively separate hydrophilic and hydrophobic particles found that contact angles of around 66° gave optimum stability. In both cases, increasing particle hydrophobicity led to partially dry coalesced froths, resulting from increased film drainage.

In flotation, the shape of particles is especially relevant, and larger, non-symmetrical particles are regularly encountered. Dippenaar (37, 38) established that "flaky" flat-type particles generally result in more stable three-phase froths with the particles aligning laterally along the contact region. It was originally reported that square-type particles (or "rhombic" type particles, such as galena) can align either laterally or diagonally, resulting in differential stability profiles, although these experiments were later repeated and the data and mechanisms involved were subject to some dispute (39). In further studies, rounded or spherical particles accomplished thinning and rupture of a liquid film in approximately 0.1 s, whereas sharp-edged particles ruptured the liquid film in only 0.02 s. Sun and Gao (40) used polytetrafluoroethylene, polyethylene and polyvinyl chloride particles (size range between 1 and 75 μm) in water/ethanol mixtures. Some of these data were explained by the effects of surface roughness, leading to "non-equilibrium" wetting behavior. Particle concentration and the state of aggregation of the particles also have been shown to be important in this study.

Most particles in nature are heterogeneous but have mostly hydrophilic (polar) surface sites which enable them to be fairly easily dispersed in water, and they do not easily adsorb on bubbles. Particles with hydrophobic surface sites are more difficult to disperse in water and are more easily agglomerated in bulk aqueous solutions. To achieve high foam stability, a critical degree of wetting (hydrophobicity) is required, so that the particles can attach to the air/solution interface, but they also need to be well dispersed in water. Several different types of surface chemical reaction have been used to create a critical balance of hydrophobic (apolar) and hydrophilic sites. With silica particles, the surface charge can be altered by the introduction of $Na^+$, $NH_4^+$ or $Al^{3+}$ ions into the lattice, or hydrophobic groups can be introduced by chemical grafting of short-chain alkyl silane or ester coupling agents. This can be achieved by liquid or vapor phase treatment, and several different types of silica-modified surfaces are illustrated in Fig. 8.16.

Silanation is frequently used in research to hydrophobize silica surfaces. Bink and coworkers (41) prepared silica particles with different degrees of hydrophobicity using this method. In a series of experiments, a relationship was established between foam stability, the residual percentage of OH groups on the particle surface after treatment and the degree of wetting (the contact angle). In these experiments the particles were dispersed in water (contained in cylindrical glass tubes) and foams generated by shaking. From the results, it was found possible to separate the dispersibility of the particles into three separate regions: high, intermediate and finally low dispersity, where the particles remained as an agglomerated powder, as indicated in Fig. 8.17(a). Foams prepared from these particles were found to be stable only in the intermediate region, where the
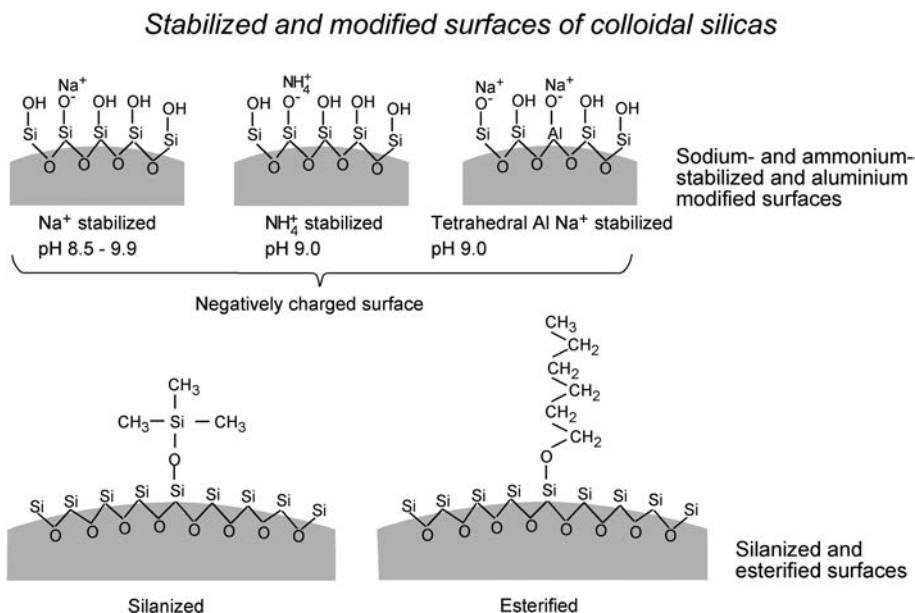
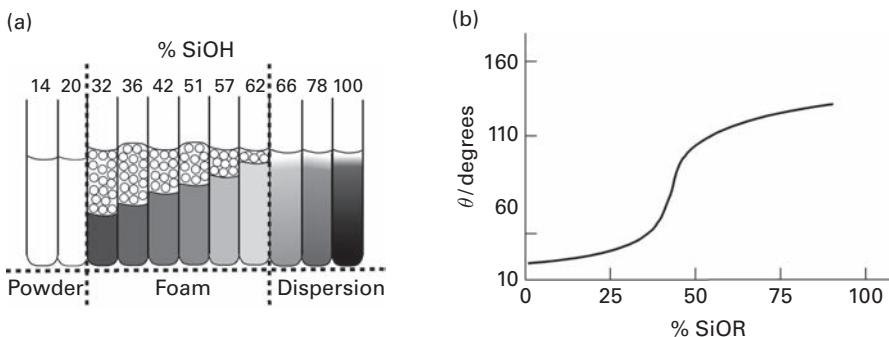**Fig. 8.16**    Stabilized and modified surfaces of colloidal silica.



**Fig.8.17**    (a) The relationship between the % SiOH groups on fumed silica particles (quasi spherical 20–30 nm diameter aggregated in 200 nm clusters) and (b) the foam stability and contact angles. Advancing contact angle of pre-water on flat surface. The % of surface SiOR groups (SiOR% = 100–SiOH%). From ref (41).

particles retained between 32 and 42% SiOH groups, and the maximum foam volume occurred at 32% SiOH level. At higher retained SiOH levels the particles were well dispersed but the system did not foam. At lower retained SiOH levels, the particles failed to disperse or to foam. In Fig. 8.17(b), the retained percent of SiOH was related to the contact angle, and it can be seen that foaming occurs between 110° and 25°.

It is of interest to note that the particles with about 32% SiOH groups which exhibited fairly high foaming performance corresponded to a contact angle of 120°. However, this value is most probably misleading since it was measured using pressed flat pellet surfaces. In fact, it is difficult to measure contact angles on small particles, and the

situation is similarly confusing in flotation experiments where high contact angles have been frequently reported for mineral particles corresponding to high foaming and flotation. These values often correspond to extremely low particle coverage, which is achieved by the chemical adsorption of hydrophobic collectors such as xanthates.

Titanium dioxide particles in the 180 nm size range have also been hydrophobized by low-temperature plasma treatment in the presence of hexa-dimethylsiloxane (a vapor-phase silane coupling agent) within a time limit ranging from 1 to 15 mins (42). This process enabled the particle to be tuned to give different degrees of hydrophobicity. Interestingly, from ESCA it was shown that hydrophobization only occurred at a small number of surface sites and the particles could be easily dispersed in water. Foaming was carried out in a cylindrical glass column under well-defined dynamic conditions at a range of gas flow rates. The foamability of the steady-state foams was found to be dependent on (a) the time of plasma treatment of the particles (surface hydrophobicity), (b) the concentration of particles in the suspension and (c) the state of dispersion of the particles.

The highest foamability was most pronounced in the neutral pH regions, where the particles had an intermediate surface charge but were fairly dispersed and the treatment time produced a critical degree of hydrophobicity. In the low pH range near the zero point of charge ($pH_{zpc}$), where the particles had a lower charge and were easily coagulated, the foamability was low. This behavior was explained by the fact that the large coagula formed in bulk solution were less easily captured by the bubbles and more easily detached from the interface (during the turbulent foaming conditions) than individual dispersed particles. In addition, low foamability also occurred at the high pH range, where the particles were found to coagulate, possibly due to the high ionic strength. This study supports earlier ideas that only moderate hydrophobicity is needed for partial coagulation of particles, thus leading to maximum foaming.

## 8.13    Janus particles

In cases where surfaces have been hydrophobically modified, usually two distinct surface regions – polar and apolar – are produced, each characterized by advancing and receding contact angles and these particles are considered as Janus particles. In the environment, many different types of amphiphilic-type particles are known to exist. For example, sludges produced from radioactive wastes often consist of noble metal oxides and hydroxides. They have a broad chemical composition and are often considered to be bi-philic. These waste systems have been studied by Wasan and coworkers (43), since they can pose problems in that they create very stable, unwanted boiling foams. Fine-tuned Janus particles can be chemically synthesized by changing the surface areas of the polar and apolar regions or by varying the strength of the hydrophobization in the apolar region. Compared with homogeneous particles, the surface activity of Janus particles (which are often considered as bifacial particles) is significantly higher. There has been

considerable interest from industry in the production and use of amphiphilic-type particles to stabilized foam systems.

## 8.14 The influence of concentration, surface charge and state of agglomeration

Surface characterization and foaming studies were carried out by Blute and coworkers (10) with nine different types of industrially manufactured, colloidal silica dispersions with particles in the nanosize region (from 5 to 40 nm). Overall, these studies confirmed earlier experiments which indicated that the foamability was critically controlled by the hydrophobicity (and hence by pH), the particle concentration, the particle size and the state of agglomeration. All the silica sols were found to have a $pH_{zpc}$ in the low region (pH 2–3) and transient foams were generated, with the hydrophobically modified particles giving the highest foamability. However, it was found that the foamability of all the sols was pH dependent, and a decrease in foamability was observed with increasing alkalinity due to the increasing negative charge at the silica surface which increased the hydrophilicity, as indicated in Fig. 8.18(a). For selected hydrophilic sols, it was also shown that the foamability increased with particle concentration (within the range of 1 to 15 wt%), as indicated in Fig. 8.18(b).

Foamability was also found to increase with decrease in particle size (within the 6 to 40 nm range). Further, foamability tests were also carried out with all the silica suspensions before and after ultrasound treatment, and it was found that the ultrasound treatment had a different effect on foamability. For the 5–9 nm particles, the foamability was reduced, but no effect was observed for the 10 nm particles. However, it was found that for the 15–40 nm sized particles, the foamability was slightly improved. This result suggested that the state of agglomeration of the particles could be important in foam generation. Foamability and foam stability were also carried out on the moderately hydrophobic modified suspensions with different solid concentrations (prepared by centrifugation), and the results verified that the particle concentration had a dominant influence on the performance. Earlier experimental
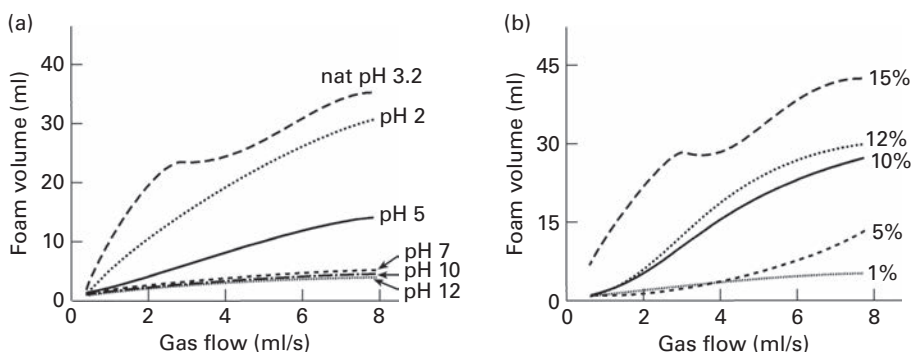
**Fig. 8.18** (a) Foamability versus pH for a commercial silica sol and (b) foamability versus particle concentration. From ref (10).

studies by Wilson (44) carried out with monodispersed latex with sizes from about 1 to 4 micron showed that the most stable froths were produced under conditions close to bulk coagulation. Armes and coworkers (45) evaluated the performance of many different types of latex systems in stabilizing foams. The effect of varying the particle size, latex concentration and latex composition of foam stability was reported. They also found that stability was influenced by the polymerization and initiator species, and highly stable foams could be produced by sterically stabilized polystyrene latex particles. It was suggested that both polydispersity and particle size were important in determining the strength and lateral ordering of the particles at the interface. SEM micrographs showed strong, ordered hexagonal networks in all stable systems with no evidence of flocculated aggregates.

## 8.15 Simple models of interactions between droplets (bubbles) coated with particles

Initially, simple theoretical models were developed, but these are mostly based on monolayer coatings of spherical partially hydrophobic particles under equilibrium conditions. A capillary pressure model was developed by Kapay (46, 47) to establish a stability criteria for two approaching bubbles (droplets), each coated with a monolayer of spherical particles or with double layers of loosely packed or clustered particles. The approach was based on the analysis of the interfacial separation pressure or force acting between the two neighboring bubbles (droplets). This total interaction was described in terms of the capillary pressure ($P_c$) or the pressure gradient between the bubbles and the inter-film fluid which was analogous to the "disjoining" pressure. As the bubble–bubble (thin film) distance is reduced, a repulsive interactions come into play. Based on a thermodynamic approach it was possible to formulate the maximum capillary pressure ($P_c^{max}$) sustainable in the thin film in relationship to the pressure needed to oppose the detachment energy of the coated film. $P_c^{max}$ was equated to the Laplace equation and various other parameters associated with changes in the structure of the film. The general equation was expressed as

$$P_c^{max} = \frac{2p_a\gamma(cos\theta + z_a)}{R_p} \tag{8.4}$$

where $R_p$ is the radius of the spherical solid particle which coats the bubble, $\gamma$ is the surface tension of the liquid in air, and $\theta$ is the contact angle of the water droplet on the solid particle in air. Parameters $p_a$ and $Z_a$ are functions of the arrangement of the particles on the bubble. Since the particle size $R_p$ is directly and inversely proportional to $P_c^{max}$, it could be suggested that smaller particles with higher curvature and more dense inter-particle packing are more effective stabilizers. Secondly, $P_c^{max}$ is directly affected by the contact angle. This leads to the assumption that the highest $P_c^{max}$ values correspond to contact angles close to zero, and the lowest values (or lowest stability) to contact

angles around 90°. More refined models were later developed to take into account the differences in particle arrangements within the cell walls and also the influence of the rigidity of packed, single-layer clusters, etc. Overall, it was concluded that the contact angle should be higher than a critical value to ensure stability, and the maximum size of particles able to stabilize foams was derived. In the majority of cases, loosely packed clusters of particles were found to be responsible for stability. However, maximum stability must also vary according to coverage, and it is important to take this into consideration in particle-stabilized foams encountered in flotation.

However, there are some general shortcomings to these theories of capillary pressure, since in addition to layers of particles, complex networks need to be considered. There is also a possibility that the drainage of fluid between bubbles can cause particles to be re-orientated or "washed away" from the interface. In addition to the work of Kapay (46, 47), alternative models have been considered. Lopetinsky and coworkers (15) considered several different types of mechanisms; these are shown in Fig. 8.19. In Fig. 8.19(a), simplified interacting bilayers are presented, and in Fig. 8.19(b), the influence of the adhesion energy which may prevent the displacement of particles from the layers is indicated. Fig. 8.19(c) shows the restriction in lateral movement caused by particle packing, which needs to be taken into consideration, and in Fig. 8.14(d), the capillary pressure resistance is indicated. Finally, in Fig. 8.19(e) the influence of the interfacial rheology in reducing drainage is suggested.
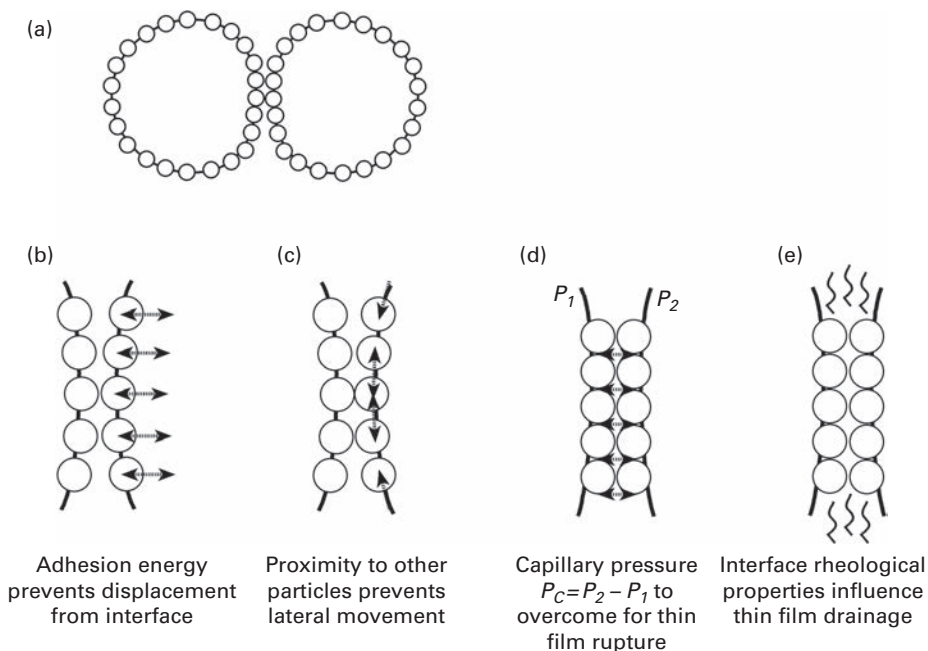


| Adhesion energy prevents displacement from interface | Proximity to other particles prevents lateral movement | Capillary pressure $P_C = P_2 - P_1$ to overcome for thin film rupture | Interface rheological properties influence thin film drainage |

**Fig. 8.19**    (a) The interaction of bilayers and (b–e) the underlying mechanisms which could be associated with stability. From ref (15).

## 8.16    Models of packing, agglomeration and bridging of particles

The amount of surface coverage can also influence the stability of the coated film. There has been considerable debate concerning the influence of the state of packing or agglomeration of particles at interfaces. In the case of higher particle concentrations, there are also indications in the literature that the interfacial stability is influenced by the formation of networks, aggregates or gels. In the case of spherical monodispersed droplets or particles, a series of different types of particle network structures, which can buildup at interfaces as envisaged by Midmore (48), are shown in Fig. 8.20

In these models, condition (a) represents a classical hexagonally close-packed (HCP) monolayer where attractive and repulsive interactions balance the network. Condition (b) represents partial flocculation where islands are shown that may occur in bulk prior to adsorption at the interface. Condition (c) represents partial flocculation occurring at low particle concentrations caused by attractive capillary forces, resulting in chain-like structures which link together, giving strong lateral stability. Finally, condition (d) represents multilayer aggregation where strong particle interface attraction dominates. Steric interactions caused by packed monolayers, clumped or aggregated coatings can result in the blockage of structures that reduce the drainage of liquid from the foam. For sparsely covered particles, the stability mechanisms are less well understood. Higher hydrophobic particles that barely enter the air/water interface can cause bridging but can also act as foam destabilizers. When considering the build-up of these structures, it is also important to take into account the magnitude of the lateral interactions such as electric double-layer repulsion and dipole–dipole repulsion, as well as van der Waals attraction and capillary forces. It is inherently difficult to provide information on the energies involved in the formation of these structures and effect of electrolytes and surfactants, particularly since some of these
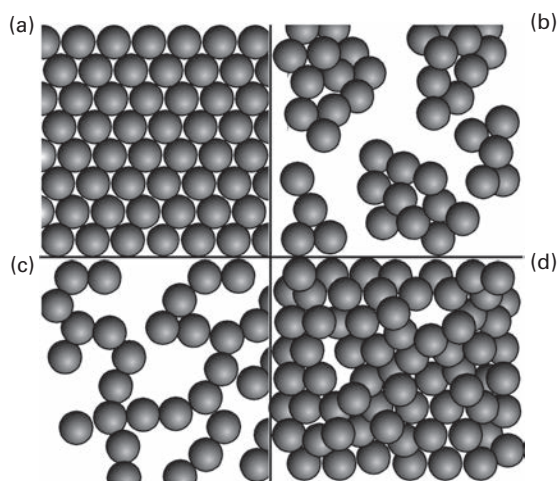


**Fig. 8.20**    Framework of possible particle network structures at the air/water interface. The particle network structures represent (a) close packing, (b) clumps, (c) lateral meso-chains and (d) aggregates. From ref (48).
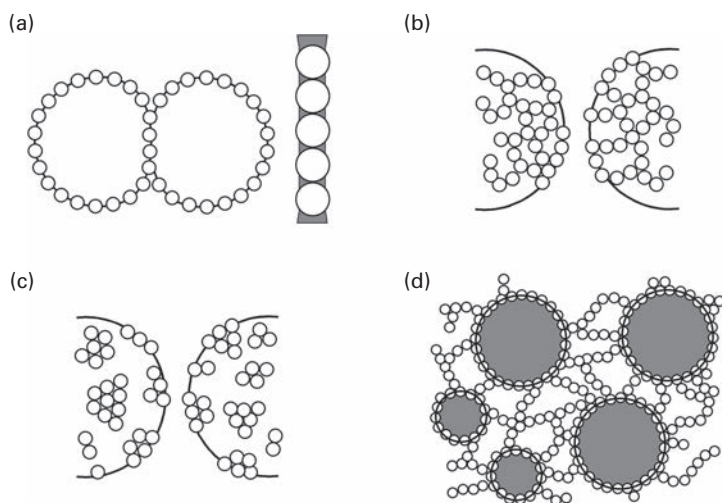
**Fig. 8.21**        Possible arrangements of particles at the droplet (bubble) interface. From ref (15).

systems are in the nano-scale range. Several experimental studies have indicated that the degree of agglomeration and structure of the agglomerates at the interface play an important role in the inter-particle steric interactions and foaming performance. This can be controlled by the adjustment of pH, electrolyte concentrations and other types of additives. The different types of structural networks, as suggested by Lopetinsky (15), that may be formed in bulk at the bubble interface are shown schematically in Fig. 8.21.

## 8.17        Particle/surfactant and particle/polymer mixtures

Synergistic effects are well known to occur in particle/surfactant mixtures; these mixtures can give enhanced foamability and foam stability over either particles or surfactants alone. In fact, this has led in some cases to the development of highly stable or super-stabilized foam systems. Clearly, there are potential benefits to be gained from synergistic action, and it occurs in many naturally occurring systems where there are different components present, for example, in colloidal food systems and flotation. Several different explanations have been put forward to account for this behavior, but it was usually found to be dependent on the particular mixed system under investigation. However, in many cases, there is evidence of unique flocculation mechanisms between particles and surfactants which may lead to the build-up of networks that could enhance bridging and steric hindrance at the contact interfaces. By analogy with chemical surfactants, there is the possibility that the particle/surfactant layer may increase the visco elasticity of the interface and cause a resistance to drainage and rupture.

Many experiments have been carried out with particles modified chemically or by physical adsorption of oppositely charged amphiphiles. This can cause marked changes in particle hydrophobicity, adsorption and flocculation behavior. Three possible effects

need to be considered: (a) changes in adsorption of surfactant on the particles which may influence hydrophobicity and contact angles (and so alter stabilization energies), (b) interactions between particle and polymer may promote partial particle flocculation and network rearrangements, both at the interface and in bulk solution and (c) surfactant/particle mixtures may cause fluctuations in interfacial tension and changes in the interfacial rheology. It is possible in some cases for all three effects to occur simultaneously or to be coupled together, and to achieve enhanced foaming characteristics a delicate balance at the particle-interface, surfactant-interface and particle-surfactant interactions is required. It is also important to consider a high particle concentration in which the excess of particles remain dispersed in the continuous phase, forming a space-filling aggregate network. For example, in the development of ceramic templates, Gonzenbach and coworkers (49) used high particle concentrations (35%) to produce stable foams which appeared to be resistant to coarsening and reduced drainage. This results in the blockage of thin film channels reducing or preventing drainage. In these studies it was also suggested that as the yield stress of the interstitial fluid increases upon confinement, gels may be produced within the lamellae films which arrest drainage.

Although cationic surfactant and silica hydrophilic nanoparticles alone generally exhibit low foaming, Binks and coworkers (50) reported a synergistic foaming effect with a mixture of silica nanoparticles and pure cationic surfactant at high pH. In this region, the coated particles were strongly negatively charged and the surfactant fully ionized with a positive charge. The synergism with this mixture was shown to be critically dependent on the ratio of the concentration of particle to surfactant. In fact, the foam stability passes through a maximum with respect to the ratio of the concentration, and these foams are remarkably stable. The dispersion stability was related to the charge on the particles. Also, adsorption isotherms of the surfactant on the surfaces of particles and relevant contact angles of water droplets at the silica surfaces were determined. It was concluded that maximum stability correlated to a strongly flocculated system with the coated particles possessing a low charge, being maximally hydrophobic and containing an adsorbed monolayer of surfactant. It was proposed that the foam stability was surfactant dominated at low surfactant concentrations, particle dominant at intermediate concentrations and finally reverted to surfactant dominant at higher concentrations. However, there was no evidence of gel formation in these systems.

Hunter and coworkers (51) studied the system octyl-grafted silica particles with a nonionic detergent-type surfactant (Triton X-100, M.W. 647) which has a hydrophilic polyethylene oxide chain with an aromatic lipophilic hydrophobic group. From surface tension and contact angle measurements it was shown that the bulk adsorption of surfactant on the particles occurs through a series of steps. At low and moderate surfactant concentration, synergism was detected and the foam stability increased by 20% compared to the pure particle system. This was explained by adsorption of hydrophobic structure on the particles causing bridging flocculation and a high-strength steric barrier preventing coalescence. At higher concentration of surfactant, which corresponded to an increase in particle coverage, the aromatic head groups of the surfactant can be re-orientated to the aqueous phase, causing the particles to become hydrophilic and resulting in a reduction of contact angles and lower foamability. The interfacial

elasticity increased with concentration, and a maximum in interfacial elasticity was detected for the composite system in the concentration range where the synergism was detected.

### 8.17.1    Surface tension measurements of particle/surfactant mixture

Surface tension experiments on mixed particle/surfactant systems have produced a broad outcome of results. Gonzenbach and Gauker (52) compared the reductions in surface tension of a short-chain fatty acid surfactant (butyric acid) with that of a mixture of the fatty acid and nano-sized aluminum oxide particles which generated high foam stability in ceramic systems. However, a high concentration of particles (35 w%) was needed to generate stable foams. The greatest reductions in surface tension were reported for butyric acid alone, and this became more pronounced with increase in fatty acid concentration. In fact, the mixtures which gave stable foam were found to be less effective in reducing the surface tension (Fig. 8.22); this indicated that surface tension was less important in stabilizing foams than in generating foams, as discussed in Chapter 1. It was theorized that the particles disrupted the adsorption equilibrium during foaming and removed free surfactant from the solution. As hydrophobized particles became attached to the bubbles, they probably collected and carried surfactant to the interface.

An interesting study was carried out by Marquez and Grady (53) in which a modified Langmuir–Blodgett (LBT) technique was used in an attempt to correlate changes in surface tension with changes in ordering of 2D structures at the air/solution interface. Both polymers and surfactants were used as spreading agents, and it was found possible in some cases to form ordered stable particle monolayers which were studied by atomic force microscope, scanning electron microscope, optical microscope and surface tension. In the case of addition of nonionic surfactant, no ordered structure was detected, which was consistent with no unique feature in surface tension results. However, for a
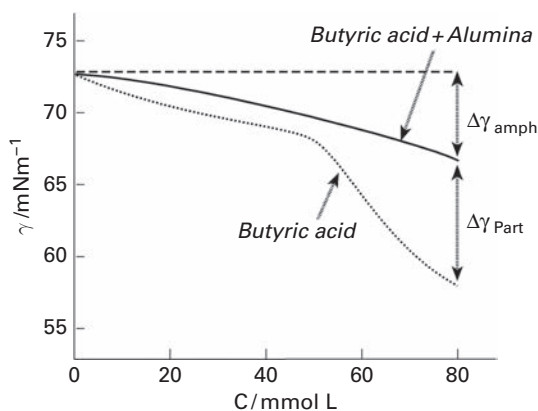


**Fig. 8.22**    Surface tension of butyric acid compared to that of butyric acid/alumina suspensions containing 35% alumina. The changes in surface tension caused by the particle and surfactant are indicated. From ref (52).

particle/surfactant mixture consisting of polystyrene (PS) latex and sodium lauryl sulfate, stable structures were detected, and it was concluded that the tensiometer combined with the LBT can be useful in determining conditions under which well-ordered latex films form on substrates. This work also suggests that structuring and re-arrangements of particles at the interface may be associated with surface tension variations. In fact, although particles may initially cause depletion of free surfactant from bulk solution, the adsorption of partially hydrophobic particles at the air/solution interface can also cause changes in surface tension.

## 8.17.2  Gel films

Although it is more or less accepted that highly flocculated systems are detrimental to foaming, many studies indicate that partially flocculated gels can give improved foaming. Most synergistic surfactant/particle mixtures show high interfacial elasticity and strong cohesive interactions and possibly gel formation. This situation is particularly relevant to protein synthesis in food systems where changes to hydrophobicity and changes in distribution of particles, surfactant and polymers in the adsorbed layer have been shown to influence the interfacial rheology (54). It has been suggested that interlocking of surfactant chains between particles may act as elastic "springs" in the layer. A suggestion for the "elastic" arrangement of particles and surfactant at an interface is shown in Fig. 8. 23.

To achieve high stability it was necessary to understand the exact balance between bulk and surface contribution. The formation of particle/surfactant or particle/polymer aggregates can cause the charge on the particles to be reduced to almost zero, thus producing strongly hydrophobic particles. This would enhance strong adsorption of the aggregate on the bubbles. At higher surfactant concentrations, a double layer of surfactant molecules forms around the particles, rendering them increasingly hydrophilic and
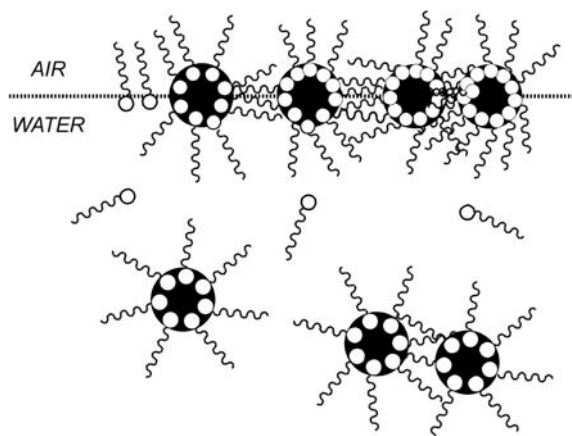


**Fig. 8.23**    Possible joint network of particles and surfactant at an interface.

reducing foaming. By fine tuning the concentrations of two species it is possible to identify different regimes of stability that correspond to coarsening and coalescence. The measurement of dilational modulus of the mixed layers was also shown to be a key component in unraveling the stability mechanism of particle/surfactant systems. Ravera and coworkers (55) carried out studies with silica nanoparticle dispersed in a solution of cetyl trimethyl ammonium bromide, and the equilibrium and dynamic interfacial tensions were measured. It was found that the enhancement of surface elasticity provides an addition mechanism that involved a synergist effect. However, in order to fully interpret the experimental data it was necessary to consider both the equilibrium and kinetic effects. Brownian motion in bulk solution appeared to play a role in the transport of the particles to the interface and the reorganization of the mixed particle/surfactant layers.

## 8.18    Diffusive disproportionation and shrinkage of particle-laden foams

Disproportionation mostly occurs in foams generated with high solubility gases such as $CO_2$ and is caused by the higher Laplace pressure in the smaller bubbles. In the case of bubbles which are coated with a low concentration of monodispersed particles, shrinkage of the bubbles can lead to a compaction of the particles at the interface into a monolayer. Provided that the particles do not become detached during compression of the monolayer, this can lead to buckling, as indicated in Fig. 8.24.

However, it was originally thought that the resulting film was unlikely to be sufficiently compact to completely resist gas diffusion, but it would most probably remain somewhat porous on a molecular level. It is well known that stabilization against disproportionation using surfactant/particle or droplet mixtures are commonly encountered in the food industry (i.e. carbonated beverages). Although these systems are partially flocculated, it could be that the coatings are less resistant to compression due to the high interfacial compression elastic modulus caused by coagulation or aggregation of the particles. Strong lateral networks at the interface are usually more effective in reducing the porosity.

Du and coworkers (56, 57) showed it was possible to stabilize air bubbles against disproportionation with nanoparticles (20 nm) in pure water but only under critical conditions. These workers used fumed silica nanoparticles which were hydrophobized with dichlorodimethylsilane to give a residual 20 to 33% coverage of SiOH groups on
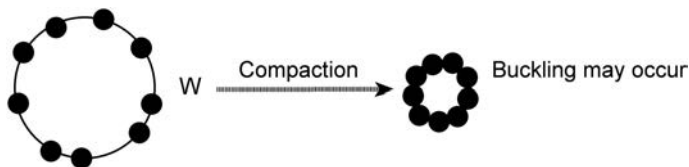


**Fig. 8.24**    Shrinking and compaction of a bubble coated with monodispersed particles during disproportionation.

the surface. Several methods were used to prepare the bubbles, including aeration, injecting the bubble beneath a surface and a pressure drop method. More extensive experiments together with a theory were documented by Dickenson and coworkers (57) in which bubbles were generated in a specially constructed cell by pressuring the aqueous phase overnight and then suddenly releasing the pressure to nucleate the bubbles within the silica dispersions. The bubbles were observed by microscope through the top of a planar interface. Although bubbles of about 250 µm radius were unstable, smaller bubbles of 50–100 µm radius were stable for several days compared to bubbles stabilized by gelatin or β-lactoglobulin proteins which shrank fairly rapidly within hours. Additional experiments using less hydrophobic fumed silica particles (67 and 89%) showed that stable foams could be generated provided a critical amount of salt was added and also by increasing the particle concentration to 1 w%. Under these critical conditions it would appear that a balance was achieved by maximizing the extent of particle adsorption and minimizing the tendency for strong aggregation in the bulk phase prior to adsorption. The results in Fig. 8.25 compare the resistance against disproportionation for partially hydrophobized silica particles in salt solution to the performance of β-lactoglobulin, where the bubbles shrink in less than 10 mins.

It was suggested that the salt increased the hydrophobicity by reducing the charge and also acted as a coagulant. Interestingly, a gel-like structure was detected on the particles which probably produced a highly compacted thin film. Excess salt would probably lead to collapse of the complete foam network rather than stabilizing individual bubbles. Foam stability is seen to drop more significantly at NaCl levels below 1 mol l$^{-1}$, relating to a "minimum" salt concentration needed for strong stability. This was not only due to the coagulation characteristics (shown by rheological measurements) but also because salt screening increased the adsorption particle contact angle. Interestingly, almost
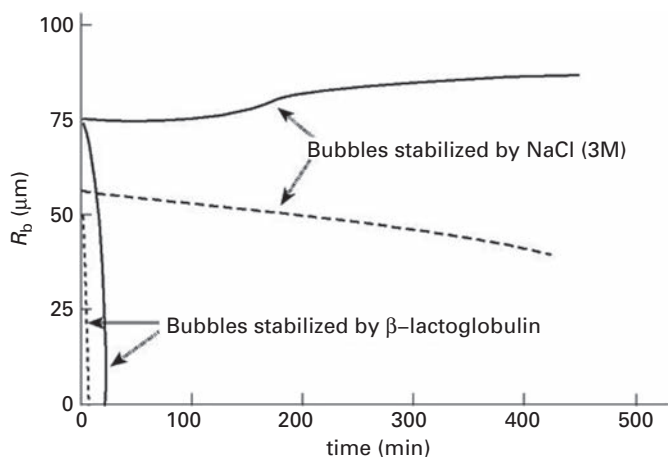


**Fig. 8.25**   Comparison of the change in bubble size ($R_b$) with time ($t$) for bubbles stabilized with 20 nm silane-treated silica particles in salt solution (3 M) with bubbles stabilized with β-lactoglobulin. From ref (57).

no stability was seen in systems without salt. Subramanian (57) modeled the effects of gas diffusion on bubbles with an arbitrary number of partially wet spheres and showed that if the local particle-laden interface could be approximated to a flat surface, it is stable to slight perturbations caused by fluctuations in the gas volume.

## 8.19    Drainage with film containing particle/surfactant mixtures

Baets (58) studied the drainage of surface-modified polystyrene particles in CTAB and observed that when the film thickness reached a particle thickness equivalent to the hydrophilic particles, they were squeezed out of the film but hydrophobic particles remained within the film, although it finally became thinner than the size of the particles. It was suggested that a bridging mechanism occurred during the drainage process. Hudales and Stein (59) found that glass particles (in the 1–10 microns size range) dispersed in a solution containing cationic surfactant retarded the drainage of thin films prepared in a glass frame and also increased foam stability.

Binks and Horozov (60) showed the influence of the hydrophobicity of silica particles (30 nm diameter) on the drainage rate. In these experiments the surface silanol content varied from 100 to 20% and aggregates were formed on the bubble surface that increased the viscosity and slowed the drainage rate. Tan and coworkers (61) studied the drainage under gravity of vertical foam films drawn on a wire frame and determined the absolute thickness using dual wavelength optical interferometry. The films were stabilized by a mixture of a nonionic surfactant (polypropylene glycol) and silica particles (0.5 $\mu$m) which had been prepared with varying degrees of hydrophobicity. From film thickness and drainage measurements, the drainage mechanism for the different types of particles could be identified. It was found that the weakly hydrophobic particles had almost no effect on drainage while highly hydrophobic particles slowed the drainage rate. The particles that were fairly hydrophobicity became attached to the interface and caused film rupture at film thicknesses in the region of about twice the particle diameter, and again bridging was suggested as a possible stabilization mechanism. However, with particles of intermediate hydrophobicity, the film lifetime increased by an order of magnitude over the hydrophilic particles, and with these dispersions, the film stability increased and the thickness was reduced to less than that of the particle diameter.

To explain these results, it was also proposed that the increase in particle hydrophobicity causes the particles to become more firmly attached to the bubbles and less mobile. With highly hydrophobic particles, film breakage operates by a dewetting bridging particle monolayer which is strongly dependent on a high contact angle. It was suggested that although hydrophobic particles were packed in the interface, some type of rearrangement could occur which was dependent on the strength of the attachment energies. This could possibly be even more important than dewetting in determining the bridging kinetics. Since the films contain numerous particles, there is a
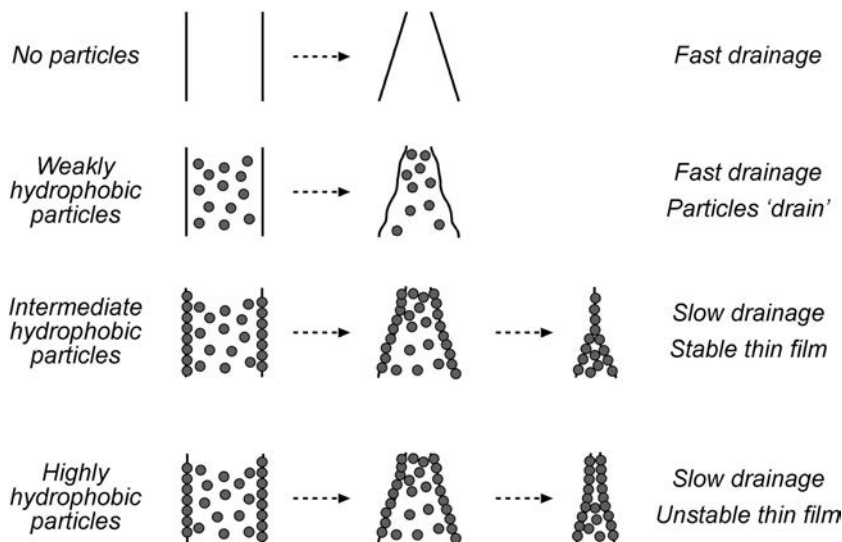
**Fig. 8.26** Schematic representation of the proposed drainage mechanisms. In the case of the particles with an intermediate degree of hydrophobicity, the slow rates of thinning were explained by rearrangement of particles and bridging across the film. From ref (61).

possibility of an exchange process involving the removal or re-attachment of particles from the central part of the film during drainage. With intermediate hydrophobic particles, the particles were less strongly attached, and this rearrangement could be sufficient to slow the drainage and prevent bridging in the film. A model suggesting the different types of drainage mechanisms for particles with different degrees of hydrophobicity is given in Fig. 8.26. Particles with intermediate and high hydrophobicity showed a tendency to become embedded in the interface.

Carn and coworkers (62) also investigated the stability of particle/surfactant mixtures using drainage experiments. This mixture consisted of silica nanoparticles (from 0.1 to 3 wt%) with high concentrations of a cationic surfactant; trimethyl tetradecyl ammonium bromide (TTAB) (> 10 CMC), and macroscopic drainage rates were measured by different methods and related to the foaming. It was reported that foam stability was strongly dependent on the particle concentration, and a strong stabilizing effect occurred at concentration of about 2 wt% which correlated with a retardation in drainage kinetics. This behavior was explained by the formation of nanoparticle/surfactant aggregates. In this first stage of drainage, the mixtures exhibited behavior similar to that for free drainage, but in the second stage of drainage, the rate was reduced and the films appeared to be stabilized by the entrapped aggregates. In fact, an insoluble cork-type structure was reported to eventually appear in the bottom node region of the thin films. This gradually blocked the Plateau borders and retarded flow. A simplified model for aggregate growth and cork formation is shown in Fig. 8.27. However, the complexes were only weakly surface active, and no reduction in surface tension was reported at low particle concentrations (< 3%).
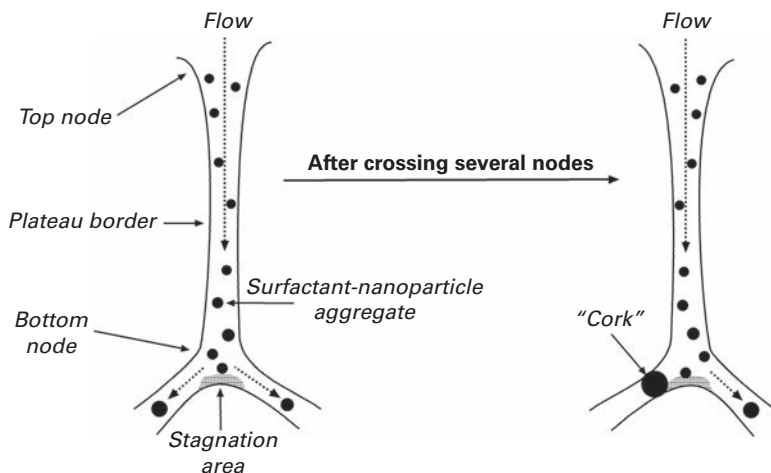
**Fig. 8.27**        Traffic jamming induced by nanoparticle surfactant flocculates in the confined geometry of a Plateau border. (a) Growing process of aggregates for low gradient of flow speed in the Plateau border section according to multiple adhesive collisions in the stagnation area in the bottom node intersection. (b) Cork formation resulting from the collision between large aggregates that may be progressively formed after crossing several node interactions. From ref (62).

## 8.20        Super particle stabilized foams generated by a magnetic field

Superstabilized bubbles and foams were generated by Lam and coworkers (63) using commercially produced nanoparticles (MAGSILICA® H8) which consist of single-domain iron oxides surrounded by a silica shell. It was found possible to generate extremely stable foams by the application of magnetic fields. The bubbles could be easily manipulated, and using a fundamental approach it was found possible to calculate the thickness of aggregated film particles attached to a bubble. The work also demonstrated that stability of the foams could be retained under well-controlled temperatures through the application of oscillating magnetic fields.

## 8.21        Preparation of stabilized monodispersed bubbles with particles

The technical difficulties associated with the preparation of foams solely by particles was discussed by Stocco and coworkers (41), together with the origin of these difficulties. A novel approach was developed by these workers based on a sonification-microfluidic technique. A gas-in-liquid slug is initially formed in a micro-channel and then subjected to cavitation at the g/l interface. Nanoparticle stabilized microbubbles are generated, and since the method uses a continuous flow system, it yields an unlimited number of gas nuclei for cavitation and a continuous production of foam with short residence time within the generator. By controlling the flow rate ratios of the gas to liquid, a high production volume with small bubble sizes can be achieved. The equipment is shown in Fig. 8.28.
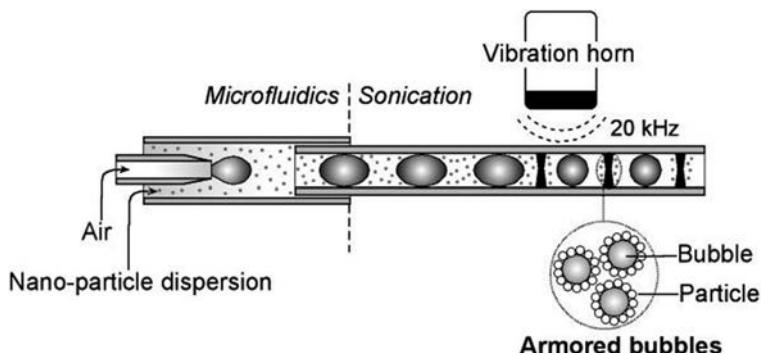
**Fig. 8.28**  Sonification-microfluidic technique for the preparation of stabilized monodispersed bubbles with particles. From ref (64).

## References

(1) A. N. Nguyen, R. J. Pugh and G. J. Jameson, *Collection and Attachment of Particles to Air Bubbles in Froth Flotation*, Chapter 9, Ed., B. P. Binks and T. Horozov, Cambridge, pp. 328–382, 2006.

(2) K. Theander and R. J. Pugh, Surface Chemical Aspects of Flotation Deinking, *Colloids Surf.*, **240**, 11–130, 2004.

(3) E. Dickenson, *Interfacial Particles in Food Emulsions and Foams*, Chapter 8, Ed. B. P. Binks and T. Horozov, Cambridge, pp. 298–327, 2006.

(4) T. N. Hunter, R. J. Pugh, G. V. Frank and G. J. Jameson, The Role of Particles in Stabilising Foams and Emulsions, *Adv. Colloid Interface Sci.*, **137**, 57–81, 2008.

(5) E. Dickinson, R. Ettelaie, T. Kostakis and B. S. Murray, Factors Controlling the Formation and Stability of Air Bubbles Stabilized by Partially Hydrophobic Silica Nanoparticles, *Langmuir*, **20**, 8517, 2004.

(6) Z. Hoffman, *Physik Chem.*, **83**, 1913.

(7) O. Bartsch, *Kolloidchemische Beihefte*, **20**, 50–77, 1924.

(8) D. M. Hausen, Diagnosis of Froth and Emulsion Problems in Flotation and Froth Extraction, *Canadian Metallurgical Quarterly*, **13**, 659–68, 1974.

(9) R. H. Ottewill, D. L. Segal and R. C. Watkins, *Chemistry & Industry*, Royal Society of Chemistry, London, 57–60, 1981.

(10) I. Blute, R. J. Pugh, J. van de Pas and I. Callaghan, Silica Nanoparticle Sols. 1. Surface Chemical Characterization and Evaluation of the Foam Generation (Foamability), *J. Colloid Interface Sci.*, **313**, 645–655, 2007.

(11) H. A. Wege, S. Kim, V. N. Paunov, Q. Zhong and O. D. Velev, Long term Stability of Foams and Emulsions with in situ formed Microparticles from Hydrophobic Cellulose, *Langmuir*, **24**, 9245–9253, 2008.

(12) H. Jin and Coworkers, Super Stable Foams Stabilized by Colloidal Ethyl Cellulose Particles, *Soft Matter*, **8** (7), 2194–2205, 2012.

(13) M. Rutland and R. J. Pugh, Calcium Soaps in Flotation Deinking; Fundamental Studies Using Surface Force and Coagulation Studies, *Colloids Surf., A*, **125** (1), 33–46, 1997.

(14)  H. J. Schultz, *Developments in Mineral Processing*, Vol. **4**, Ed. D. W. Fuerstenau, Elsevier, 1983.

(15)  R. J. G. Lopetinsky, J. H. Masliyah and Z. Xu, *Solid Stabilized Emulsions: a Review in Colloidal Particles at Liquid Interfaces*, Ed. B. P. Binks and T. Horozov, Cambridge, pp. 186–224, 2006.

(16)  I. Blute I, R. J. Pugh, J. van de Pas and I. Callaghan, Industrial Manufactured Silica Nanoparticle Sols – Generation and Stability Part 2: Surface Tension, Particle Concentration and Foamability, *Colloids Surf., A*, **337** (1–3), 127–135, 2009.

(17)  T. Okubo, Surface Tension of Structured Colloidal Suspensions of Polystyrene and Silica Spheres at the a/w Interface, *Int. J. Colloid Interface Sci.*, **171**, 55–62, 1995.

(18)  L. Dong and D. T. Johnson, The Study of the Surface Tension of Charged Stabilized Colloidal Dispersions, *J. Dispersion Sci. Technol.*, **25**, 575–583, 2005; L. Dong and D. Johnson, Surface Tension of Charged Stabilized Colloidal Suspensions at the Water/Air interface, *Langmuir*, **19**, 10205–10209, 2003.

(19)  K. Carlsson and D. Johnson, Surface Tension Driven Flow due to the Adsorption and Desorption of Colloidal Particles, *J. Colloid Interface Sci.*, **242**, 279–283, 2001.

(20)  S. Levine, B. D. Bowen and S. J. Partridge, Stabilization of Emulsion by Fine Particle: Partitioning between Continous Phase and Oil/Water Interface, *Colloids Surf.*, **38**, 325–343 and Capillary and van der Waal Forces between Particles, 345–364, 1989.

(21)  P. A. Kralchevsky, N. D. Denkov and K. D. Danov, Particles with an Undulated Contact Line at a Fluid Interface: Interactions between Capillary Quadrupoles and Rheology of Particulate Monolayers, *Langmuir*, **17**, 7694–7705, 2001.

(22)  P. A. Kralchevsky and N. D. Denkov, Capillary Forces and Structuring in Layers of Colloidal Particles, *Curr. Opin. Colloid Interface Sci.*, **6**, 383–401, 2001.

(23)  J. Lucassen, Capillary Forces between Solid Particles in Fluid Interfaces, *Colloids Surf.*, **65**, 131–137, 1992.

(24)  P. Pieranski, 2D Interfacial Colloidal Crystals, *Phys. Rev. Lett.*, **45**, 569–572, 1980.

(25)  A. Moncho-Jorda, E. Martinez-Lopez, A. E. Gonzalez and R. Hidalgo-Alvarez, Role of Long Range Repulsive Interactions in 2D Colloidal Aggregation, *Langmuir*, **18**, 9183, 2002.

(26)  A. I. Abdel-Fattah and M. S. El-Genk, On Colloidal Particles Sorption onto a Stagnant Air/Water Interface, *Adv. Colloid Interface Sci.*, **78**, 237–266, 1998; A. I. Abdel-Fattah and M. S. El-Genk, Sorption of Hydrophobic Negatively Charged Microspheres onto a Stagnent Air/Water Interface, *J. Colloid Interface Sci.*, **202**, 417–429, 1998.

(27)  D. F. Williams and J. C. Berg, Dynamic Wetting in Low Capillary Number Regime, *J. Colloid Interface Sci.*, **152**, 218–229, 1992.

(28)  R. Aveyard, J. H. Clint, D. Nees and V. N. Paunov, Compression and Structure of Monolayers of Charged Latex Particles at the a/w and Octane/w Interface, *Langmuir* **16**, 1969–1979, 2000.

(29)  D. J. Robinson and J. C. Earnshaw, Initiation of Aggregation in Colloidal Particle Monolayers, *Langmuir*, **9**, 1436–1438, 1993.

(30)  F. Ghezzi, J. C. Earnshaw, M. Finnis and M. McCluney, Pattern formation in Colloidal Monolayers at the Air/Water Interface, *J. Colloid Interface Sci.*, **238**, 433–446, 2001.

(31)  I. Blute, R. J. Pugh, J. van de Pas and I. Callaghan, Silica Nanoparticle Sols. Part 3: Monitoring the State of Agglomeration at the Air/Water Interface, *J. Colloid Interface Sci.*, **336**, 584–591, 2009.

(32)  R. G. Alargova and Coworkers, Foam Superstabilization by Polymer Micro-rods, *Langmuir*, **20**, 10371–10374, 2004.

(33)  W. Zhou and Coworkers, How Rigid Rods Self-Assemble at Curved Surface, *Angew. Chem. Int. Ed.*, **48**, 378–381, 2009.

(34)  G. Johansson and R. J. Pugh, Influence of particle size and hydrophobicity on the stabilization of mineralized froths, *Int. J. Miner. Process.*, **31**, 1992.

(35)  S. Schwarz and S. Grano, Effect of Particle Hydrophobicity on Particle and Water Transport across a Flotation Froth, *Colloids Surf., A*, **256**, 157–164, 2005.

(36)  S. Ata, N. Ahmed and G. J. Jameson, Collection of Hydrophobic Particles in the Froth Phase, *Int. J. Miner. Process.*, **64**, 101–122, 2002; S. Ata, N. Ahmed and G. J. Jameson, The Effect of Hydrophobicity on the Drainage of Gangue Minerals in Flotation Froths, *Miner. Eng.*, **17**, 897–901, 2004.

(37)  A. Dippenaar. The Destabilization of Froths by Solids, 1. The Mechanism of Film Rupture, *Int. J. Miner. Process.*, **9**, 1–14, 1982.

(38)  A. Dippenaar, The Destabilization of Froths by Solids, 1. The Rate Determining Step, *Int. J. Miner. Process.*, **9**, 15–22, 1982.

(39)  G. D. M. Morris and J. J. Cilliers, Behaviour of a Thin Film Revisited, Dippennar, *Int. J. Miner. Process.*, **1**–6, 131, 2014.

(40)  Y. Q. Sun and T. Gao, The Optimum Wetting Angle for the Stabilization of Liquid-Metal Foams by Experimental Simulation, *Metall and Materials, Trans A*, **30** (10), 3285–3292, 2002.

(41)  A. Stocco, E. Rio, B. P. Binks and D. Langevin, Aqueous Foams Stablilized Soleby by Particles, *Soft Matter*, **7**, 1260–67, 2011.

(42)  R. J. Pugh, Foaming in Chemical Surfactant Free Aqueous Dispersions of Anatase (Titanium Dioxide) Particles, *Langmuir*, **23**(15), 7972–7980, 2007.

(43)  S. K. Binal and Coworkers, Foaming in simulated Radioactive Waste, *Environ Sci.*, **35**, 3941–47, 2001; D. T. Wasan, A. D. Nikolov, P. Kralchevski and I. Ivanov, Universality in Film Stratification due to Colloidal Crystals Formation, *Colloids Surf.*, **67**, 139–145, 1992.

(44)  J. Wilson, *A Study of Particulate Foams*, Ph. D. thesis University of Bristol, 1981.

(45)  S. Fujii, P. D. Iddon, A. J. Ryan and S. P. Armes. Aqueous Particulate Foams Stabilized Solely with Polymer Latex Particles, *Langmuir*, **22**, 7512–7520, 2000; S. Fujii, A. J. Ryan and S. P. Armes, Long Range Structure Order, Moire Patterns and Iridescence in Latex Stabilized Foams, *J. Am Chem. Soc.*, **128**, 7882–7886, 2006.

(46)  G. Kaptay and Coworkers, *Metal Foams and Porous Metal Structures*, MIT Pubishing, Bremen, Germany, 1999; G. Kaptay. Interfacial Criteria for Stabilization of Liquid Foams by Solid Particles, *Colloids Surf., A*, **230**, 67–80, 2003.

(47)  G. Kaptay, On the Equation of the Maximum Capillary Pressure Induced by Solid Particles Stabilized by Emulsions and Foams, *Colloids Surf., A*, **282**/283, 387–401, 2006.

(48)  B. R. Midmore, Effect of Aqueous Phase Composition on the Properties of Silica Stabilized w/o Emulsions, *J. Colloid Interface Sci.*, **213**, 352–359, 1999.

(49) U. T. Gonzenbach, A. R. Studart, E. Tervoort and L. J. Gauckler, Stabilization of Foams with Inorganic Particles, *Langmuir*, **22** (26), 10983–10988, 2006.

(50) B. P. Binks, M. Kirkland and J. A. Rodrigues, Origin of Stabilisation of Aqueous Foams in Nanoparticle–Surfactant Mixtures, *Soft Matter*, **4**, 2373–2382, 2008.

(51) T. Hunter, E. J. Wanless, G. J. Jameson. and R. J. Pugh, Nonionic Surfactant Interactions with Hydrophobic Nanoparticles: Impact on Foam Stability, *Colloids Surf., A*, **347**, 81–89, 2009.

(52) U. T. Gonzenbach, A. R. Studart, E. Tervoort and L. J. Gauckler, Unstable Particle-Stabilized Foams, *Angew. Chem. Int. Ed.*, **45**, 3526–3530, 2006.

(53) M. Marquez and B. P. Grady, The Use of Surface Tension to Predict the Formation of 2D Arrays of Latex Particles via Langmuir Blodgett-like Technique, *Langmuir*, **20**, 10998–11004, 2004.

(54) B. S. Murray, Interfacial Rheology of Food Emulsifiers and Proteins, *Curr. Opin. Colloid Interface Sci.*, **7**, 426–431, 2002.

(55) F. Ravera, E. Santini, G. Loglio, M. Ferrari and L. Liggieri, Effect of Nanoparticles on the Interfacial Props of the Liquid/Liquid and Liquid/Air Surface Layers, *J. Phys. Chem. B*, **110**, 19543–19551, 2006.

(56) Z. Du, M. P. Bilbao-Montoya, B. P. Binks, E. Dickinson, R. Ettelaie and B. S. Murray, Outstanding Stability of Particle Stabilized Bubbles, *Langmuir*, **19**, 3106–3108, 2003.

(57) E. Dickinson, R. Ettelaie, B. S. Murray and Z. Du, Kinetics of Disproportionation of Air Bubbles beneath a Planar Interface, *J. Colloid Interface Sci.*, **252**, 202–213, 2002; Z. Du, M. P. Bilbao-Montoya, B. P. Binks, E. Dickinson, R. Ettelaie and B. S. Murray, Outstanding Stability of Particle Stabilized Bubbles, *Langmuir*, **19**, 3106–3108, 2003.

(58) P. J. M. Baetes, *Foam Films Drawn from Dispersions*, Eindhoven University of Tech, Eindhoven, Netherlands, 1993.

(59) J. B. M. Hudales and H. N. J. Stein, The Influence of Solid Particles on Foam and Film drainage, *J. Colloid Interface Sci.*, **140**, 307, 1990.

(60) B. P. Binks and T. S. Horozov. Angewandte Chemie, *International Edition*, **44**, 3722–3725, 2005.

(61) S. N. Tan, Y. Yang and R. G. Horn, Thinning of a Vertial Free-Draining Aqueous Film Incorporating Colloidal Particles, *Langmuir*, **26** (1), 63–73, 2009.

(62) F. Carn and coworkers, Foam Drainage in the Presence of Nanoparticles-Surfactant Mixtures, *Langmuir*, **25** (14), 7847–7856, 2009.

(63) S. Lam, E. Blanco S. K. Smoukov, K. P. Velikov and O. D. Velev, Magnetically Responsive Pickering Foams, *J. Am. Chem. Soc.*, **133** (35), 13856–13859, 2011.

(64) H. Chen, J. Li, W. Zhou, E. G. Pelan, S. D. Stoyanov, L. N. Arnaudov and H. A. Stone, Sonication-Microfluidics for Fabrication of NanoParticle-Stabilized Microbubbles, Eurofoam Thessaloniki, *Greece, Oral Presentation*, **25**, 2014.